NON CONTACT VIBRATION CONTROL SYSTEM WITH LINEAR ACTUATOR USING PERMANENT MAGNET

Phaisarn Sudwilai

A dissertation submitted to
Kochi University of Technology
In partial fulfillment of the requirements
for the degree of

Doctor of Philosophy

Graduate School of Engineering
Kochi University of Technology
Kochi, Japan

September 2012

NON CONTACT VIBRATION CONTROL SYSTEM WITH LINEAR ACTUATOR USING PERMANENT MAGNET

Phaisarn Sudwilai

A dissertation submitted to
Kochi University of Technology
In partial fulfillment of the requirements
for the degree of

Doctor of Philosophy

Graduate School of Engineering
Kochi University of Technology
Kochi, Japan

September 2012

Abstract

A noncontact vibration control using permanent magnet system is supporting system without mechanical contacts, there is suitable in the process of plating, coating or rolling of steel sheets, this research is to develop a new non-contact vibration control system using linear actuator and permanent magnet. This research proposes a vibration suppression mechanism consisting of permanent magnets, actuators, sensors and a controller. The dissertation aims to design new system is to reduce vibration and/or deformation of thin steel sheets by controlling the air-gap between the permanent magnets and the steel sheets.

In this dissertation, the first proposed the feedback control of the system was designed by means of the LQR (Linear Quadratic Regulator) method. In this study, the proposed vibration suppression mechanism was designed, the prototype was constructed for experimental confirmations, feasibility of the model of prototype and the design of the controller was analyzed, and numerical simulations and experimental examinations were carried out to verify the effectiveness of the controller designed by LQR method. The simulations and experiments for impulse response were performed under the following system conditions: 1) without feedback control, 2) without feedback control and permanent magnet, 3) with feedback control when the feedback control designed using LQR method and gains set to LQR1, 4) with feedback control when the feedback control designed using LQR method and the gains set to LQR2 and 5) with feedback control when the feedback control designed using LQR method and the gains set to LQR3. According to frequency response, the system were performed to suppress disturbance force in vary frequency such as 5, 29 and 59 rad/sec under the following system conditions: 1) without feedback control, 2) without feedback control and permanent magnet, 3) with feedback control when the feedback control designed using LQR method and gains set to LQR1, 4) with feedback control when the feedback control designed using LQR method and the gains set to LQR2 and 5) with feedback control when the feedback control designed using LQR method and the gains set to LQR3. All results verified that the system effectively suppressed vibration.

Finally, the feedback control of the system was designed using H_{∞}LSDP (loop shaping design procedure) method. In this study, the design of the controller was analyzed, and numerical simulations and experimental examinations were carried out to

verify the effectiveness of the controller designed by H_{∞}LSDP method. The simulations and experiments were performed under the following system conditions: 1) without feedback control, 2) without feedback control and permanent magnet, 3) with feedback control when the feedback control designed using LQR method and gains set to LQR1 and 4) with feedback control when the feedback control designed using H_{∞}LSDP method. According to frequency response, the system were performed to suppress disturbance force in vary frequency such as 5, 29 and 59 rad/sec under the following system conditions: 1) without feedback control, 2) without feedback control and permanent magnet, 3) with feedback control when the feedback control designed using LQR method and gains set to LQR1 and 4) with feedback control when the feedback control designed using H_{∞}LSDP method. All results verified that the system effectively suppressed vibration.

Table of Contents

Lists of Figures

Lists of Tables

Chapter 1

Generation introduction

1.1 Background

The steel sheets are widely use in many industrial company such as automobile bodies, electrical appliances and household products as shown in Figs. 1.1 and 1.3. These sheets are produced through a rolling process with the flexible sheet supported by roller and prone to vibration. This vibration leads to surface degradation as shown in Fig. 1.2. Due to this, a vibration suppressor with mechanical contact is not suitable as a countermeasure.

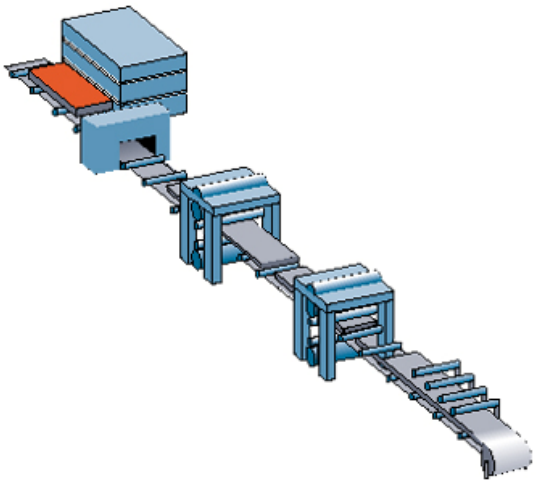

http://www.hsnee.com/rolling_mill.htm

Fig. 1.1 Process of Rolling-Mill

Objects are easily damaged due to their material makeup when they have just been rolled, coated or plated. Therefore, a noncontact suppression mechanism is more suitable for controlling the minimization of deformation of the steel sheets and can

minimize such problems. Noncontact vibration control methods which use attractive force of electromagnets have been already proposed [1]-[4], [14]. The principal weakness of these methods is that the control range is very constricted, because the attractive force of the magnet varies in inverse proportion to the square of air-gap length. If the vibration amplitude of the object is large, minimizing deformation by means of electromagnets is ineffective for the control of the object. On the other hand, a control method using permanent magnets located at the desired iron sheet passage has also been proposed [5]. However, this method uses passive control and can not be successfully suppressed under large disturbances as shown in Fig. 1.2 (b).

A noncontact suspension system using permanent magnets and linear actuators has been proposed [6]. The key element of the design is the force control mechanism. A linear actuator drives a permanent magnet and varies the air-gap between the magnet and the object. Variation of the size of the air-gap changes the attractive force. Here the vibration control system uses this type of force control mechanism for vibration suppression, since the control range is almost the same as of the actuator stroke length. In this system vibration control range is expected to be correspondingly wide.

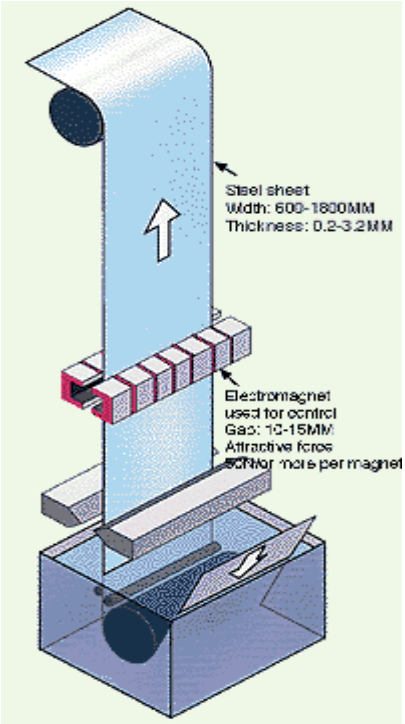

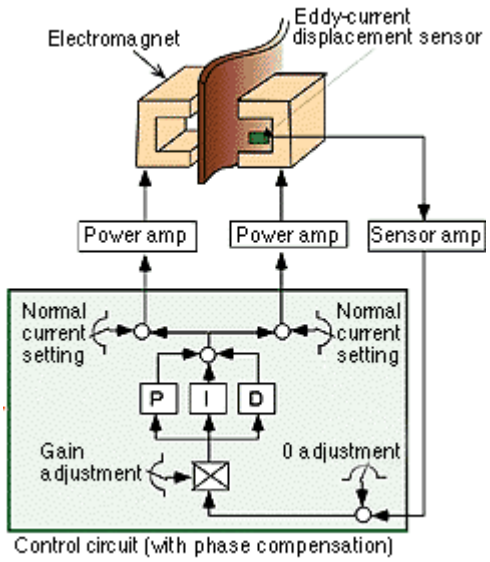

http://www.shinko-elec.co.jp/NewsReleases/new_18.htm

(a) **(b)**

Fig. 1.2 Industrial process of Rolling mill and coating

1.1.1 Application of vibration control system

There are many application of noncontact vibration control system, such as in commercial process, thin steel sheets rolling, coating and plating as shown in Fig. 1.3 and 1.4 [41]-[42].

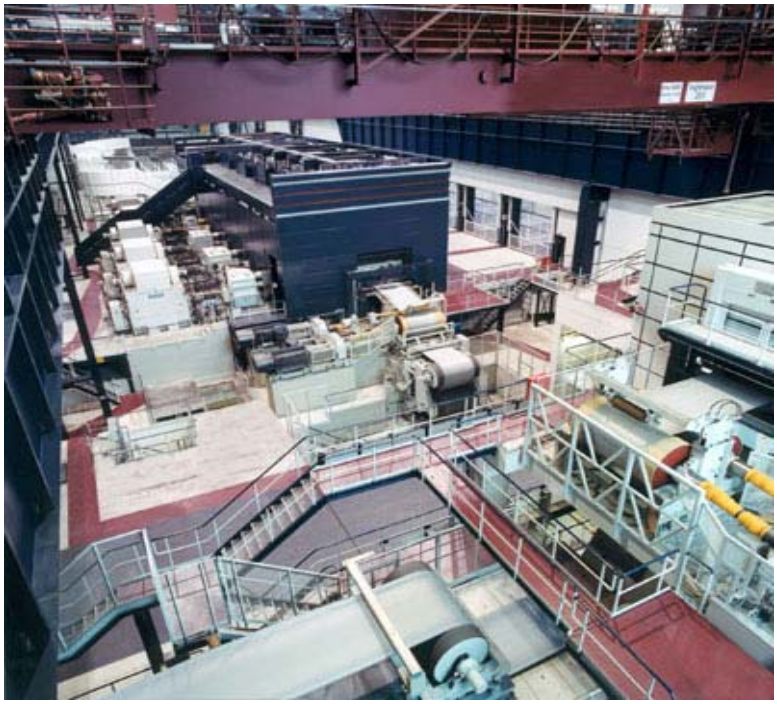

http://www.hsnee.com/rolling_mill.htm

Fig. 1.3 Industrial process of Rolling-mill

http://51ppgi.com/ral-3020-traffic-red-colour-coated-steel-coil-185/

Fig. 1.4 Industrial process of Rolling mill and coating

1.2 Motivation, goals and control method

1.2.1 Motivation

The purpose of this research is to develop a new vibration control system with linear actuator using permanent magnet. It can realize noncontact active control. It can be applied in industrial process such as automobile bodies, electrical appliances and numerous household products.

1.2.2 Goals

Firstly, applied the linear control theory examines the feasibility of the vibration control system. Based on the considerations of above, the research project will aim at making to reduce the vibration signal of the object.

1.2.3 Control method

Adjusting the attractive force of permanent magnet acting to vibration object by control air-gap between permanent magnet and vibration objected.

Firstly, apply the feedback controller that design by means of LQR method to the system [7]-[13]. The testing of feedback control is on simulation and experiment. The condition of test is impulse response, step response and frequency response.

Finally, another one of controller will design for improve the uncertainly model, H_∞ loop shaping control is apply to the system [21]-[24]. The testing of the controller is also on simulation and experiment. The condition of test is impulse response, step response and frequency response.

1.3 Structure of thesis

This chapter that deals with the background and the goal and motivation of this investigation is the part of this thesis.

The chapter 2 presents the vibration suppression technique. This chapter commences by illustration of plating process in commercial process. Following is the principle of operation of vibration control system in the independent drive type. The principle of operation of the simultaneous drive type is. The result of force testing of permanent magnet and vibration body in the same condition with the system prototype when the

equilibrium position of the vibration body and permanent magnet are set to 12.5 and 20.0 mm, respectively.

The chapter 3 presents of vibration control system model, system linearized, and state space model of the system prototype. In this chapter commences by over view of the vibration suppression mechanism in view point of block diagram. The system prototype is shown. Finally, this chapter shows the details and symbols of the vibration control equation. The block diagram in the last section shows the transfer function and state space model.

The chapter 4 presents the LQR technique applied for the vibration control system, feedback control designing, numerical simulation via MATLAB with Simulink in various conditions such as impulse response, step response and frequency response. The chapter initially by reviews the linearized system. The numerical simulation and experimental results were performed under various conditions such as impulse response, step response and frequency response, respectively.

The chapter 5 presents the H_∞ Loop Shaping technique using a Loop Shaping Design Procedure (LSDP). The LSDP is modern H_∞ optimization approach, suitable for multivariable, robustness and based on concepts from classical Bode plot methods. This chapter begins by the linearized model of vibration control system. The procedure of LSDP approach in vibration control system. Finally, shows the numerical simulation and the experiment results.

The chapter 6 presents the conclusions of the dissertations. The conclusion consists of the LQR technique applied for the vibration control system and the H_∞ Loop Shaping technique using a Loop Shaping Design Procedure (LSDP). Finally, this chapter gives the recommendation of the dissertations.

Chapter 2

Vibration suppression mechanism

2.1 Introduction

This chapter presents the vibration suppression technique. This chapter commences by illustration of plating process in commercial process. Following is the principle of operation of vibration control system in the independent drive type. The principle of operation of the simultaneous drive type is. The result of force testing of permanent magnet and vibration body in the same condition with the system prototype when the equilibrium position of the vibration body and permanent magnet are set to 12.5 and 20.0 mm, respectively.

2.2 Illustration of plating process

A schematic diagram of a vibration suppression mechanism for plating or coating process is shown in Fig.2.1 The steel sheet is fed from the right side of the figure and is directed upwards by a roller. While the steel sheet is being fed into the solution bath, plating or coating is carried out. After the plating process is completed, the steel is seasoned or cooled in a vertical feed. During the seasoning process, the steel is especially sensitive to deformation. Consequently vibration control in the seasoning process is very important.

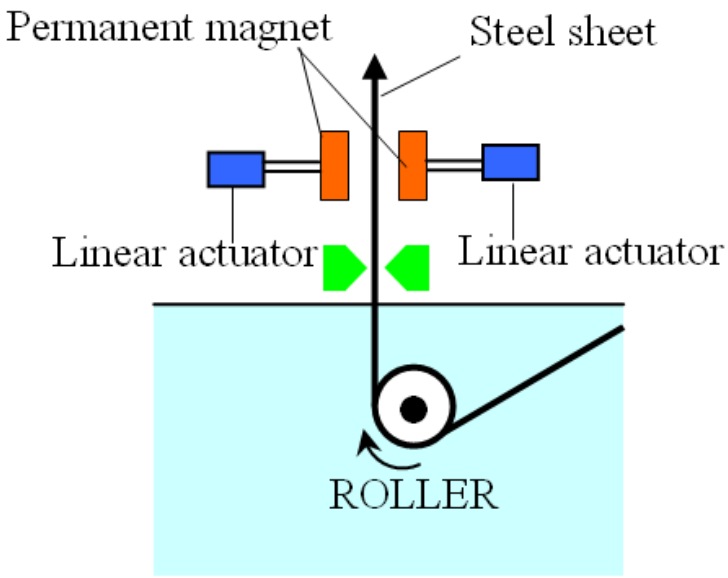

Fig. 2.1 Illustration of plating process

In this research, a new type of vibration suppression mechanism, as shown in Fig. 2.1 is proposed. The mechanism consists of two permanent magnets, two linear actuators, sensors which measure the steel sheet displacement, and a controller. The sensors and controller are omitted in the figure. The intention of the system is to reduce vibration caused by the roller feed mechanism, air wipers, and high speed plating. Air wipers, represented by the green element in the figure, adjust the thickness of the plating.

2.3 Method of controlling

The design of the prototype of vibration suppression mechanism is illustrated in Fig. 2.2. In this figure, the vertical sheet in the center represents the steel sheet and is labeled “Vibration body”. The magnets on both sides are driven in the horizontal direction by actuators, which are labeled “VCM”.

The principle of the vibration suppression method is as follows. When the vibration body swings to the right of the equilibrium position, as shown in Fig.2.2 (a1), the left actuator (VCM) drives the left magnet to the right, the displacement between the left magnet and vibration body is reduced, and the left attractive force becomes larger. Consequently, the magnetic force caused the vibration body return to the original

equilibrium position. Similarly, when the vibration body swings to the left, as shown in Fig. 2.2 (b1), the right actuator drives the right magnet to the left, the attractive force on the right side of the vibration body becomes larger and this force caused the object to return to the equilibrium position. The attractive force of the permanent magnet can suppress vibration and deformation of the object.

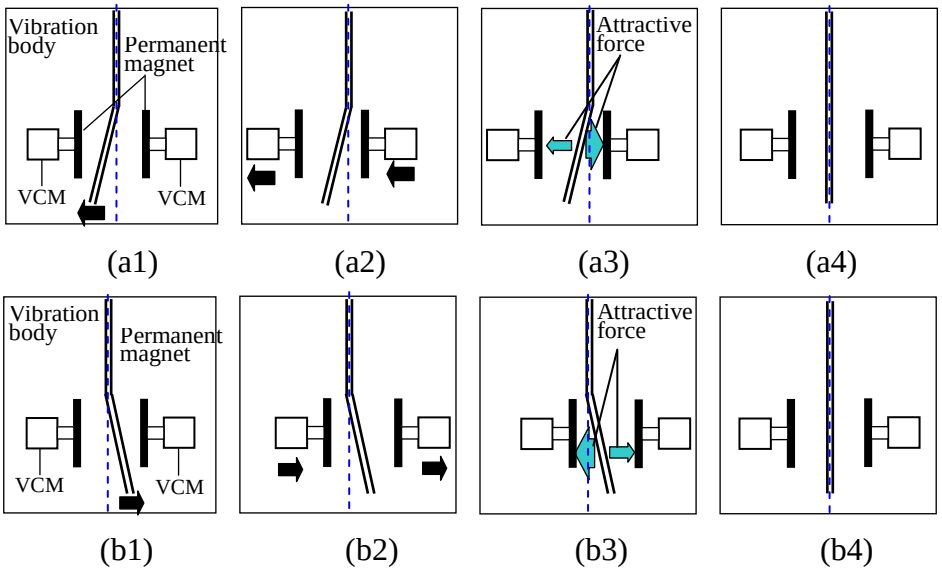

(a1)-(a4) Vibration body swing to the right

(b1)-(b4) Vibration body swing to the left

Fig. 2.2 Method of controlling vibration in case of independent drive type

Figure 2.3 shows the simultaneous drive type, system that is a little different from the principal system shown in Fig. 2.2. This prototype is, however, the first step for the proposed system. There is no problem for verifying the feasibility.

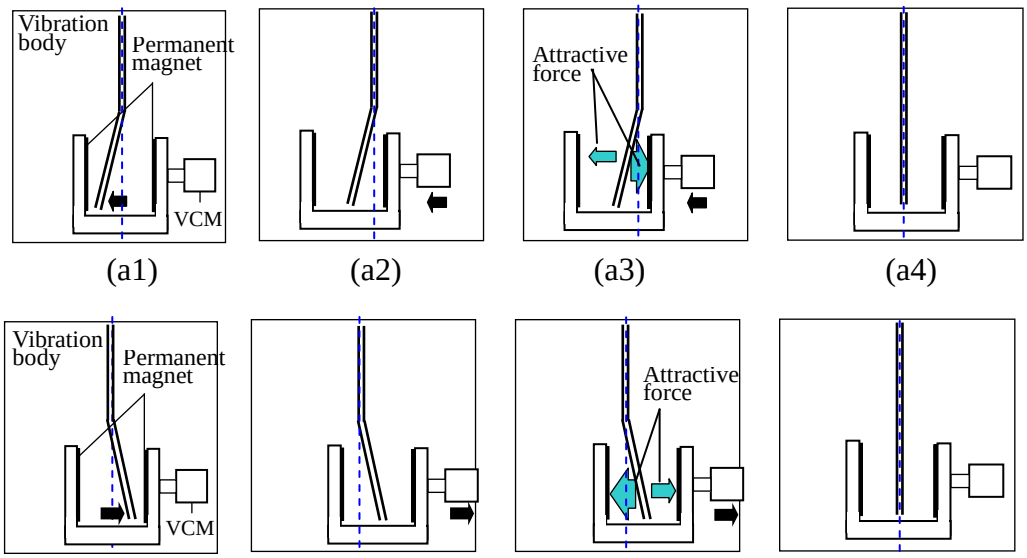

(a1)-(a4) Vibration body swing to the right

(b1)-(b4) Vibration body swing to the left

Fig. 2.3 Method of controlling vibration in case of simultaneous drive type

2.4 The relationship between force and displacement

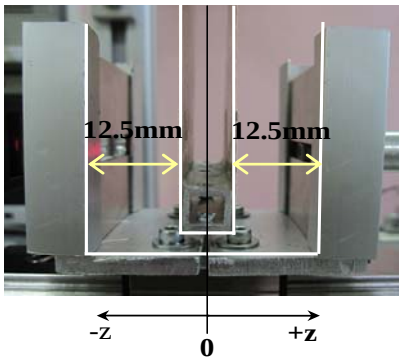

Fig. 2.4 The air-gap with the equilibrium position set to 12.5 mm

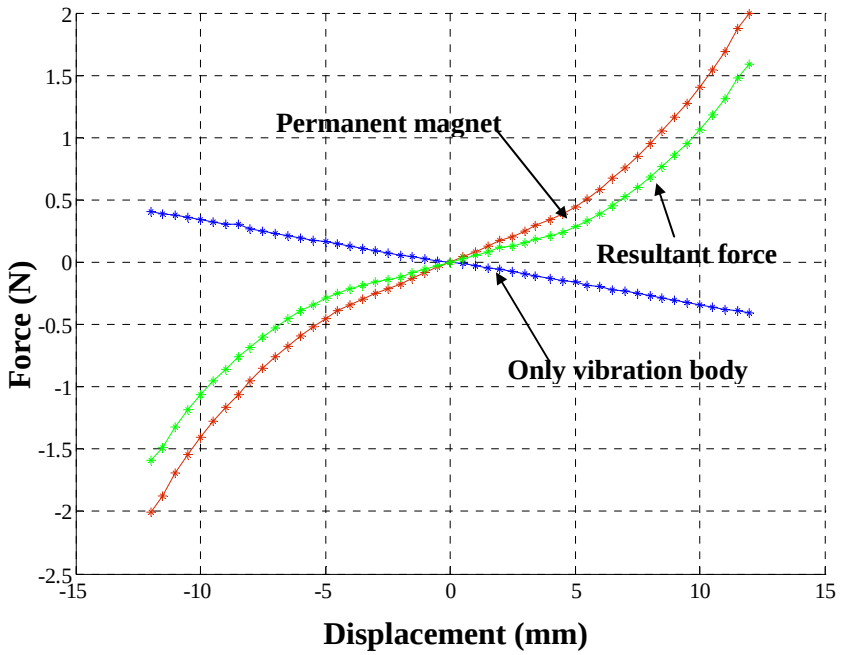

Fig. 2.5 The relationship between the attractive force of the permanent magnet, the force of the vibration body, the resultant force and the air-gap with the equilibrium position set to 12.5 mm

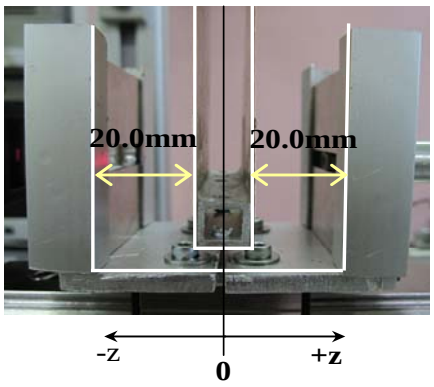

Fig. 2.6 The air-gap with the equilibrium position set to 20 mm

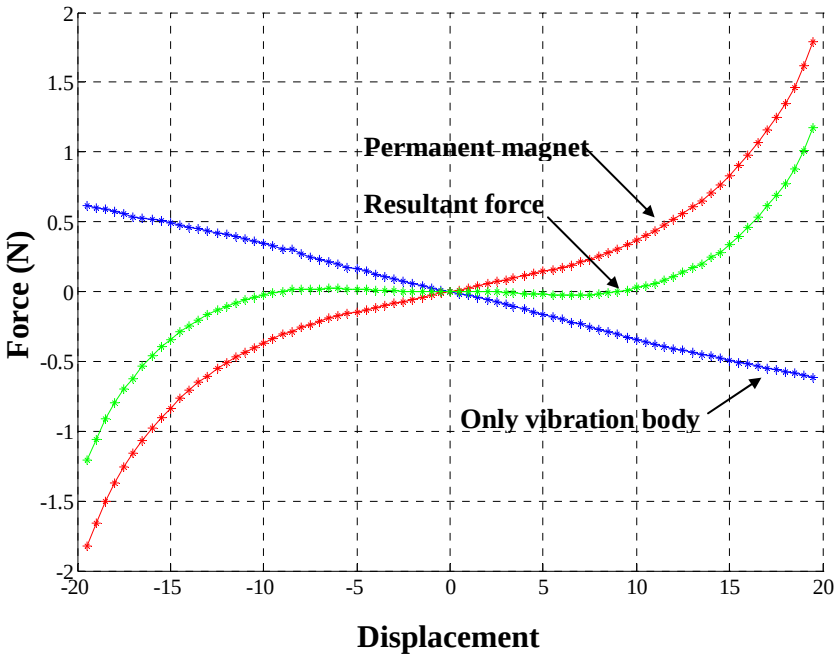

Fig. 2.7 The relationship between the attractive force of the permanent magnet, the force of the vibration body, the resultant force and the air-gap with the equilibrium position set to 20.0 mm

Figure 2.4 and 2.6 shows the construction of permanent magnet that setup to a slider the equilibrium position of air gap between permanent magnet and parallel phosphor bronze plate set to 12.5 and 20 mm, respectively.

Figure 2.5 and 2.7 show the relationship between the attractive force of the

permanent magnet and force of the vibration body, the resultant force when the air gaps are set to 12.5 and 20 mm, respectively.

2.5 The disturbance force

The disturbance force is generated by DC motor with install to the vibration body as shown in Fig.2.8. In this figure it can be seen that when DC motor rotate it make vibration vibrate in sinusoidal signal. The relationship between the DC voltage supply of the DC motor and frequency of the disturbance force as shown in Fig. 2.9.

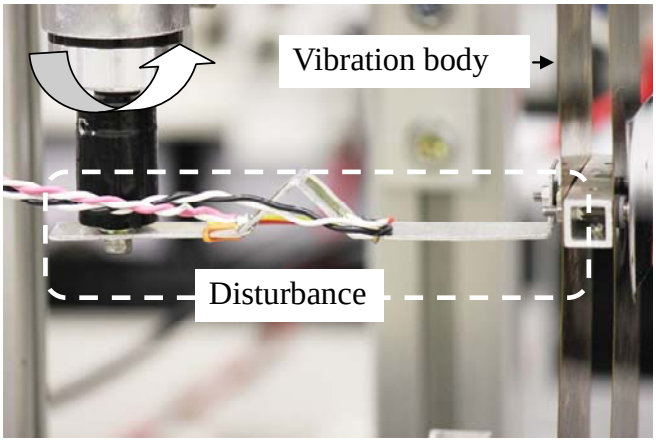

Fig. 2.8 The photograph of disturbance

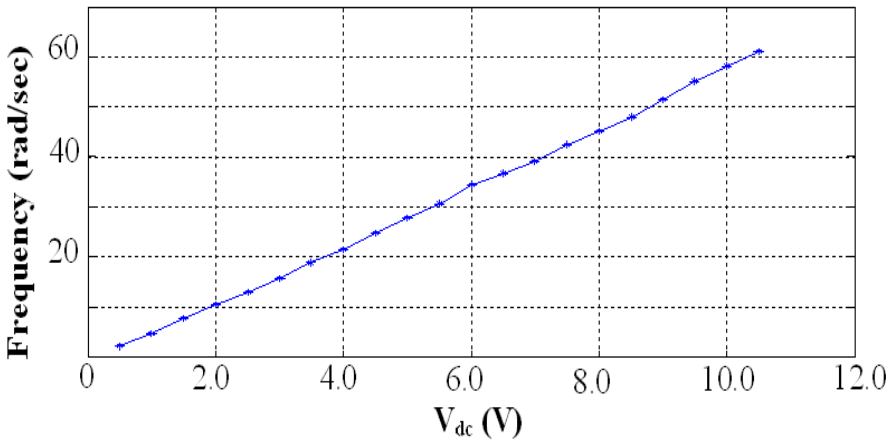

Fig. 2.9 The relationship between the dc-voltage supply and the dc motor and the frequency of the disturbance force

Chapter 3

System modeling

3.1 Introduction

This chapter presents the system modeling of the vibration suppression mechanism. In this chapter commences by over view of the vibration suppression mechanism in view point of block diagram. The system prototype is shown.

Finally, this chapter shows the details and symbols of the vibration control equation. The block diagram in the last section shows the transfer function and state space model.

3.2 Block diagram of vibration control system

The control system block diagram is shown in Fig. 3.1. As seen in the figure, the controller is using DSP. It calculates the generating force of the VCM from two displacement sensor signals and the output is current signal for the amplifier, before amplifier the current command signal is filtered. The amplifier changes the command signal to the current for the VCM and the VCM changes the currents to the force action to slider proportionally. For DSP programming, MATLAB with SIMULINK and Pass/C67 were used.

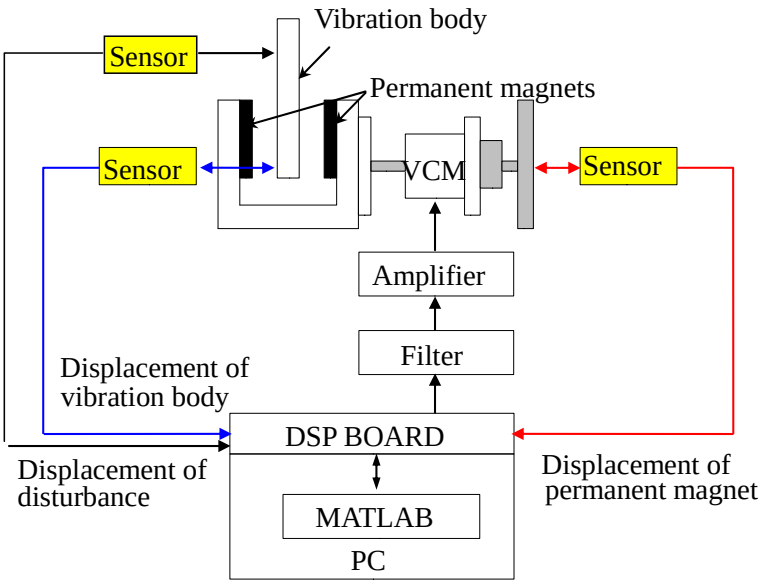

Fig. 3.1 Block diagram of vibration control system

3.3 System prototype

An experimental system to examine the performance of the proposed vibration control mechanism was manufactured. The photograph of the system is shown in Fig. 3.2. The system consists of a vibration body, two permanent magnets installed with a slider, a voice coil motor (VCM), displacement sensors and force sensor.

The vibration body is structured as a parallel spring made by phosphor bronze (50x190 mm) and installs steel plates (25x50 mm) on the both sides facing to the permanent magnets. Two permanent magnets are installed on the slider driven by the voice coil motor (VCM). The system is a simultaneous drive system that is a little different from the principal system shown in Fig. 2.3 This prototype is, however, the first step for the proposed system. There is no problem for verifying the feasibility. Three sensors are installed for measuring the displacements of the vibration body, displacement of disturbance and displacement of the slider. A laser sensor is used for the motion of the vibration body and an eddy current sensor is used for the motion of magnets which is the same as the VCM movement and disturbance.

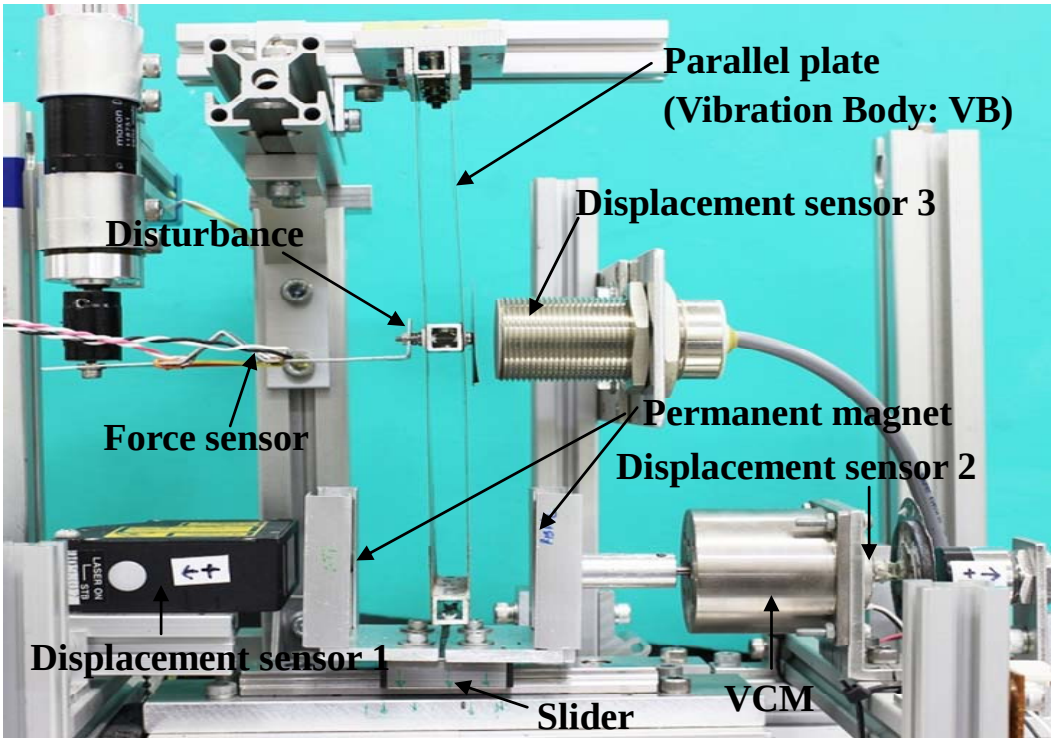

Fig. 3.2 Photo of system prototype

3.4 System modeling

This system was modeled in order to analyze the system, to adopt the linear control theory, and to synthesize the control system. For modeling, the specifications should be figured out. Other specification values of the prototype are indicated in Table 3.1.

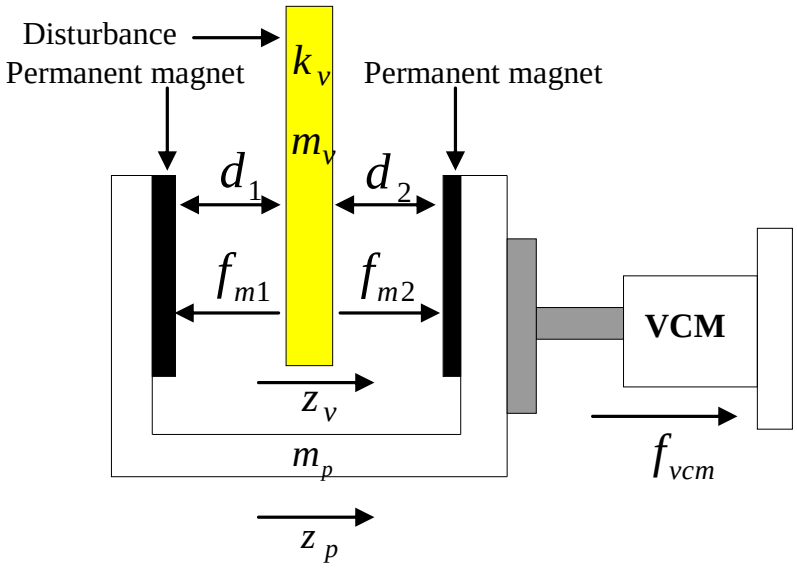

Fig. 3.3 System modeling

In the model, the motion of the vibration body, as supported by a parallel spring is assumed to be translational. An illustration of the model is shown in Fig. 3.3.

The symbols used in the model are as follows:

z_v : displacement of the vibration body

z_p : displacement of the permanent magnet

d_1 : the air gap length between the left permanent magnet and the vibration body

d_2 : the air gap length between the right permanent magnets and the vibration body

d_0 : the air-gap length when the vibration body is centred between the magnets

f_{m1} : the attractive force of the left permanent magnet

f_{m2} : the attractive force of the right permanent magnet

f_m : the resultant force of the magnets

f_{vcm} : the actuator generating force

f_d : the disturbance force

c_v : the damping coefficient of the vibration body

c_p : the damping coefficient of the permanent magnet

k_v : the parallel spring constant

k_p : the permanent magnet constant

m_v : the equivalent mass of the vibration body

m_p : the mass of the permanent magnet together with the voice coil motor (VCM) and the slider.

The specification values of the prototype are indicated in Table 3.1

The attractive force of the permanent magnet is

$$f_{m2} = \frac{k}{(d_2 - z_v + z_p)^2} \tag{3.1}$$

$$f_{m1} = \frac{k}{(d_1 + z_v - z_p)^2} \tag{3.2}$$

The resultant force is assumed to be inversely proportional to the square of the gap length.

$$f_m = f_{m2} - f_{m1} \tag{3.3}$$

$$f_m = \frac{k}{(d_2 - z_v + z_p)^2} - \frac{k}{(d_1 + z_v - z_p)^2} \tag{3.4}$$

where k is constant, by linearization of the attractive force of the magnets, the resultant force can be represented by

$$\tilde{f}_m = k_m(z_v - z_p) \tag{3.5}$$

where k_m is a constant value and the motion equation of the vibration body is

$$m_v z_v'' = -k_v z_v - c_v z_v' + f_m + f_d \tag{3.6}$$

The motion equation of the slider is

$$m_p z_p'' = -k_p z_p - c_p z_p' + f_{vcm} - f_m \tag{3.7}$$

From the motion equation of the vibration body in Eqs.(3.6), the Laplace transform of this equation is

$$m_v s^2 Y_v(s) + c_v s Y_v(s) + k_v Y_v(s) = F_v(s) \tag{3.8}$$

$$F_v(s) = F_m(s) + F_d(s) \tag{3.9}$$

$$Y_v(s)(m_v s^2 + c_v s + k_v) = F_v(s) \tag{3.10}$$

$$\frac{Y_v(s)}{F_v(s)} = \frac{1}{m_v s^2 + c_v s + k_v} \tag{3.11}$$

Similarly of the motion equation of vibration body, the motion equation of permanent magnet become

$$m_p s^2 Y_p(s) + c_p s Y_p(s) + k_p Y_p(s) = F_p(s) \quad (3.12)$$

$$F_p(s) = F_{vcm}(s) - F_m(s) \quad (3.13)$$

$$Y_p(s)(m_p s^2 + c_p s + k_p) = F_p(s) \quad (3.14)$$

$$\frac{Y_p(s)}{F_p(s)} = \frac{1}{m_p s^2 + c_p s + k_p} \quad (3.15)$$

Substitute Eq. (3.5) into Eqs. (3.6) and (3.7) become

$$m_v z_v'' = -k_v z_v - c_v z_v' + k_m(z_v - z_p) + f_d \quad (3.16)$$

$$m_p z_p'' = -k_p z_p - c_p z_p' + f_{vcm} - k_m(z_v - z_p) \quad (3.17)$$

The inputs of the system are defined as the forces of the actuator (VCM) f_{vcm} and the disturbance f_d. The outputs are the displacement of the vibration body z_v and the slider z_p. The model can be represented by Eqs. (3.1), (3.2) and (3.3).

The system can be represented by the block diagram shown in Fig. 3.4. There are two controllers in the loops of the vibration body and the magnets. A state space model can be derived from Eqs. (3.4) – (3.6) as

$$x' = Ax + B_1 u_1 + B_2 u_2, \quad .(3.18)$$

$$y = Cx, \quad (3.19)$$

where

$$A = \begin{bmatrix} 0 & 1 & 0 & 0 \\ \frac{k_m - k_v}{m_v} & -\frac{c_v}{m_v} & -\frac{k_m}{m_v} & 0 \\ 0 & 0 & 0 & 1 \\ -\frac{k_m}{m_p} & 0 & \frac{k_m - k_p}{m_p} & -\frac{c_p}{m_p} \end{bmatrix}$$

$$b_1 = \begin{bmatrix} 0 \\ 0 \\ 0 \\ \frac{1}{m_p} \end{bmatrix}$$

$$b_2 = \begin{bmatrix} 0 \\ \frac{1}{m_v} \\ 0 \\ 0 \end{bmatrix}$$

$u_1 = f_{vcm}$

$u_2 = f_d$

$$y = \begin{bmatrix} z_v \\ z_p \end{bmatrix}$$

$$x = \begin{bmatrix} z_v \\ z_v' \\ z_p \\ z_p' \end{bmatrix} \tag{3.20}$$

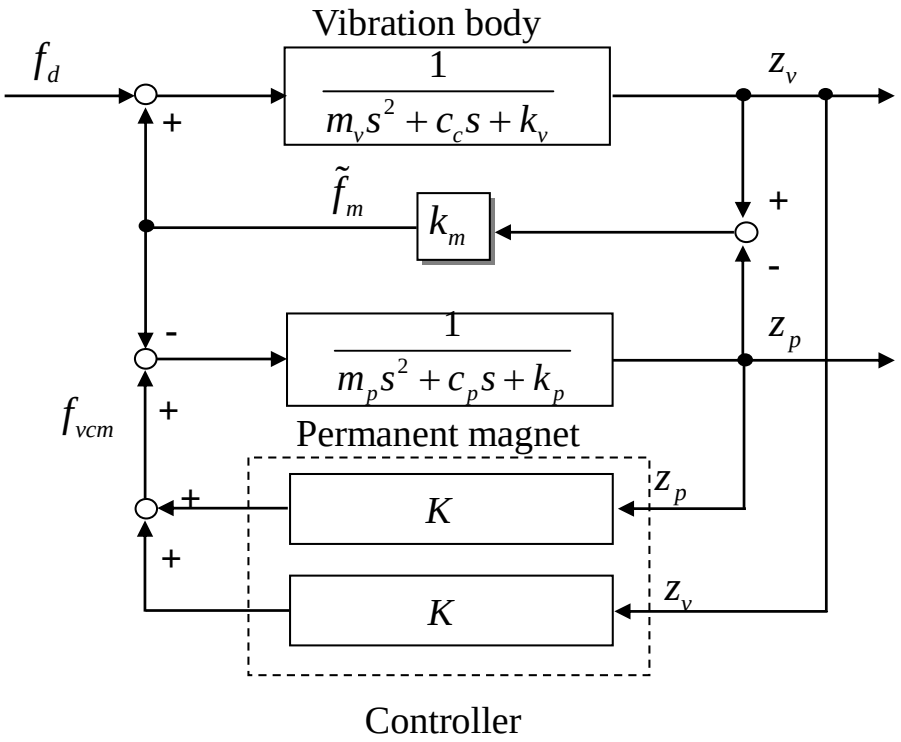

Fig. 3.4 Block-diagram of a vibration control system

Table 3.1 Parameters of the vibration control system.

c_v : damping coefficient of the vibration body	0.02 Ns/m
c_p : damping coefficient of the permanent magnet	0 Ns/m
k_v : constant of vibration body	150 N/m
k_p : constant of permanent magnet	0 N/m
m_v : mass of vibration body	0.047 kg
m_p :mass of permanent magnet	0.292 kg
k_m : constant of linearization	33.85 N/m

Chapter 4

Linear Quadratic Regulator (LQR) Approach

4.1 Introduction

This chapter presents the feedback controller of vibration control system, the controller was designed by means of Linear Quadratic Regulator (LQR) method[24]. The linear modeled of vibrant control system. The chapter initially by reviews the linearized system.

The numerical simulation and experimental results were performed under various conditions such as impulse response, step response and frequency response, respectively.

4.2 Linear Quadratic Regulator (LQR) Approach

According to the equation of attractive force of permanent magnet as shown in equation (3.4), by linearization of the attractive force of the magnets, the resultant force can be represented by

$$\tilde{f}_m = k_m(z_v - z_p), \tag{4.1}$$

where k_m is a constant value and equation (3.6) and (3.7) become

$$m_v z_v'' = -k_v z_v - c_v z_v' + k_m(z_v - z_p) + f_d, \tag{4.2}$$

$$m_p z_p'' = -k_p z_p - c_p z_p' + f_{vcm} - k_m(z_v - z_p) \tag{4.3}$$

The system can be represented by the block diagram shown in Fig. 4.1. There are PD controllers in the loops of the vibration body and the magnets. The feedback gains are calculated by means of the LQR control theory. Using the LQR method, a state space model can be derived from Eqs. (3.5),(3.6) and (3.7) as

$$x' = Ax + B_1 u_1 + B_2 u_2 , \tag{4.4}$$

$$y = Cx , \tag{4.5}$$

where

$$A = \begin{bmatrix} 0 & 1 & 0 & 0 \\ \frac{k_m - k_v}{m_v} & -\frac{c_v}{m_v} & -\frac{k_m}{m_v} & 0 \\ 0 & 0 & 0 & 1 \\ -\frac{k_m}{m_p} & 0 & \frac{k_m - k_p}{m_p} & -\frac{c_p}{m_p} \end{bmatrix}$$

$$b_1 = \begin{bmatrix} 0 \\ 0 \\ 0 \\ \frac{1}{m_p} \end{bmatrix}$$

$$b_2 = \begin{bmatrix} 0 \\ \frac{1}{m_v} \\ 0 \\ 0 \end{bmatrix}$$

$u_1 = f_{vcm}$

$u_2 = f_d$

$$y = \begin{bmatrix} z_v \\ z_p \end{bmatrix}$$

$$x = \begin{bmatrix} z_v \\ z_v' \\ z_p \\ z_p' \end{bmatrix} \tag{4.6}$$

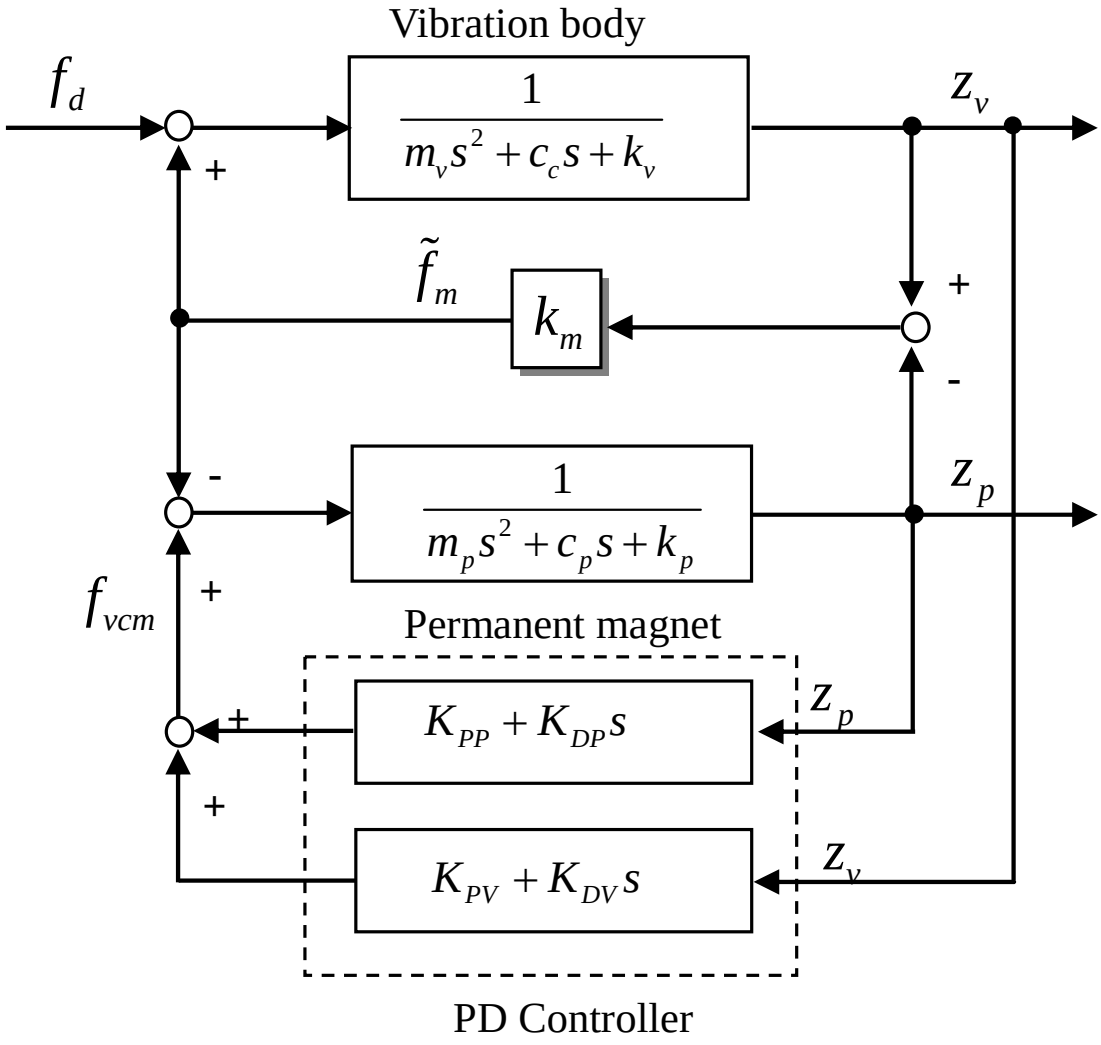

Fig. 4.1 Block-diagram of a vibration control system

The LQR can be used to get the feedback gains. The relationship between attractive force of permanent magnet and feedback gains as shown in equation (4.7) [6]-[7]. Based on the characteristics of the system, we examined the weighting matrix Q and input weighting matrix R as following:

$$f_{vcm} = -(k_{PV} z_v + k_{DV} z_v' + k_{PP} z_p + k_{DP} z_p') \tag{4.7}$$

For The feedback system LQR1 uses the weighting matrix Q_1 of

$$Q_1 = \begin{bmatrix} 1\times10^{10} & 0 & 0 & 0 \\ 0 & 1 & 0 & 0 \\ 0 & 0 & 1\times10^{3} & 0 \\ 0 & 0 & 0 & 1 \end{bmatrix}, \tag{4.8}$$

The system LQR2 uses the matrix Q_2 of

$$Q_2 = \begin{bmatrix} 1\times10^{9} & 0 & 0 & 0 \\ 0 & 1 & 0 & 0 \\ 0 & 0 & 1\times10^{3} & 0 \\ 0 & 0 & 0 & 1 \end{bmatrix}, \tag{4.9}$$

And the system LQR3 uses the matrix Q_3 of

$$Q_3 = \begin{bmatrix} 1\times10^{8} & 0 & 0 & 0 \\ 0 & 1 & 0 & 0 \\ 0 & 0 & 1\times10^{3} & 0 \\ 0 & 0 & 0 & 1 \end{bmatrix} \tag{4.10}$$

Using MATLAB software, the feedback gain *K* is calculated as following:

K_1=[-6.3e4 -1.7e3 1.6e4 96] (4.11)

K_2=[-1.2e4 -660 8.5e3 71] (4.12)

K_3=[96 -224 4.4e3 51] (4.13)

4.3 Simulation Results

For feasibility study, numerical simulations carried out with the non linearization of the attractive force. The simulations are examined in the following cases.

Case 1: impulse response when the system without feedback control.
Case 2: impulse response, the system conditions are following:
1) without feedback control,
2) with feedback control, gains set to LQR1,
3) with feedback control, gains set to LQR2 and
4) with feedback control, gains set to LQR3.
Case 3: frequency response, the frequency of disturbance force set to 5, 29 and 59 rad/sec and the system conditions are following:
1) without feedback control,
2) with feedback control, gains set to LQR1,
3) with feedback control, gains set to LQR2 and
4) with feedback control, gains set to LQR3.

The simulations were carried out using the calculated feedback gains in the three cases. In the simulations, the feedback controls in the loop are set to K_1 for LQR1, K_2 for LQR2 and K_3 for LQR3, respectively.

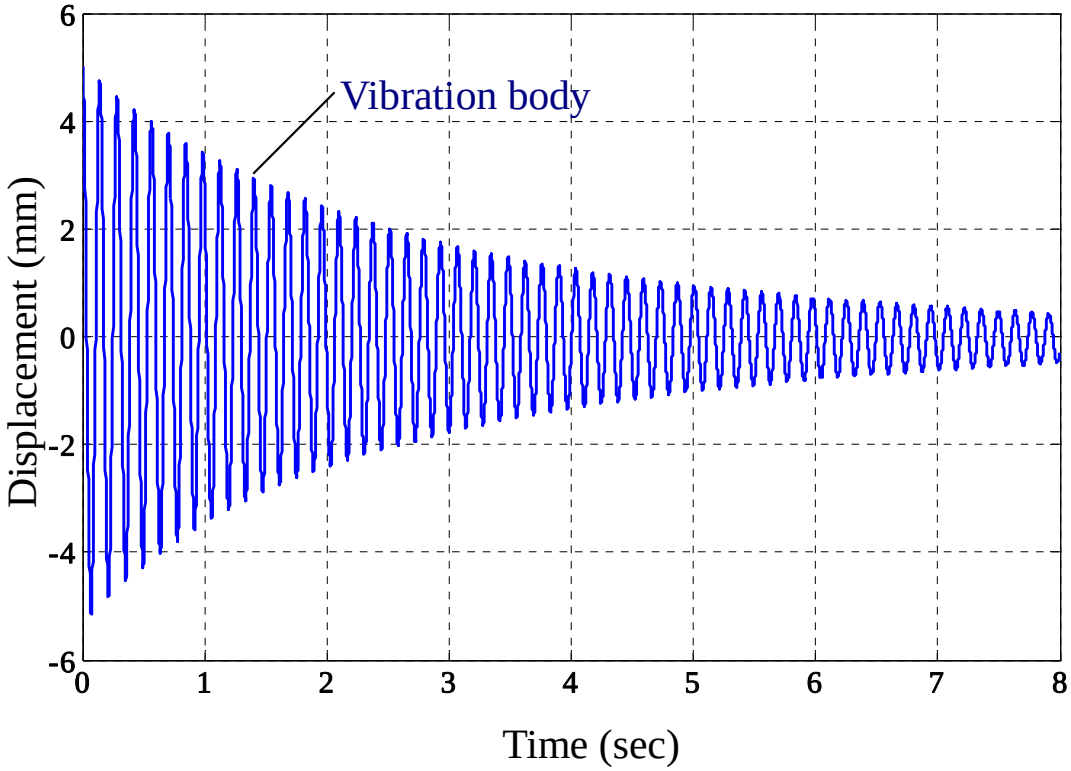

Fig. 4.2 Simulation result of displacement signal of the vibration body, the following system conditions: 1) impulse response and 2) without feedback control.

Figure 4.2 shown the displacement signal from the vibration body when the system without control, it can be seen that the system vibrate in sinusoidal function and oscillate reach to stop in the equilibrium position. As the result, the vibration body need time more than 8 second to stop vibrate.

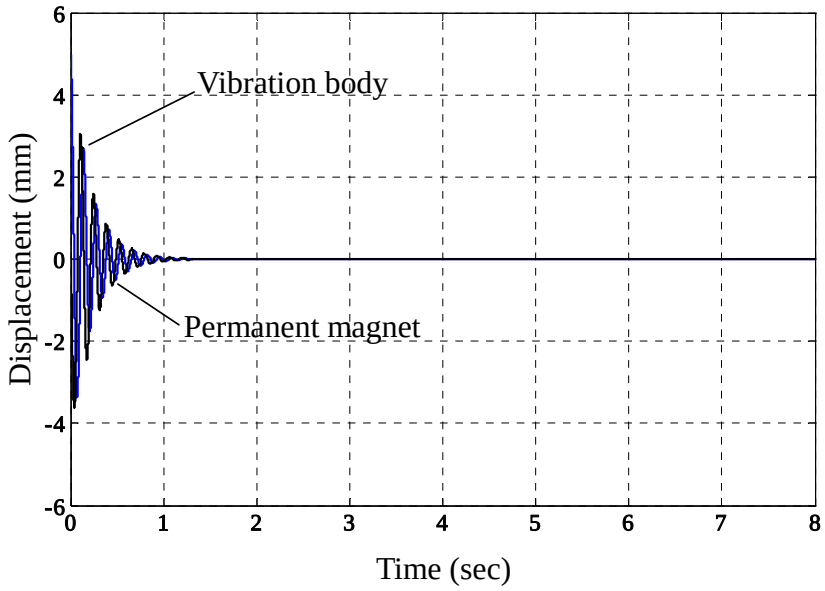

(a)

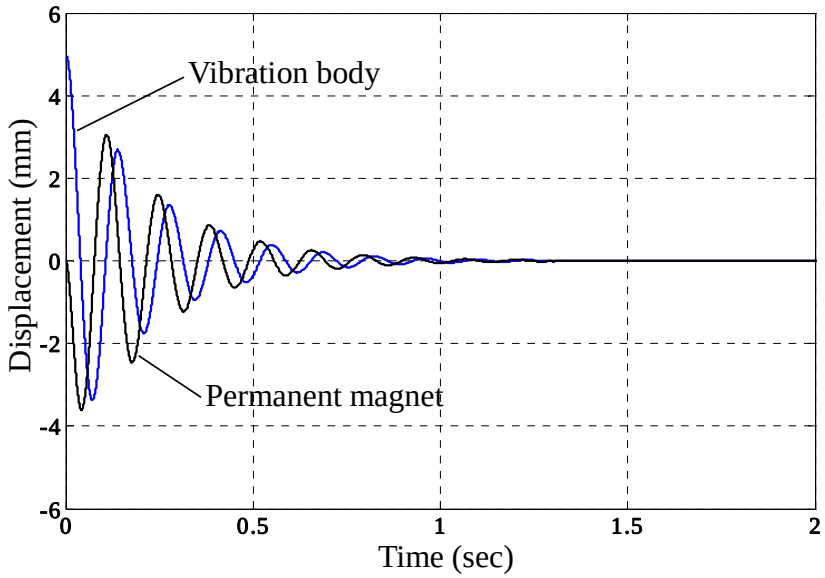

(b)

Fig. 4.3 Simulation result of displacement signal of the vibration body and permanent magnet, the following system conditions: 1) impulse response and 2) with feedback control, gains set to LQR1

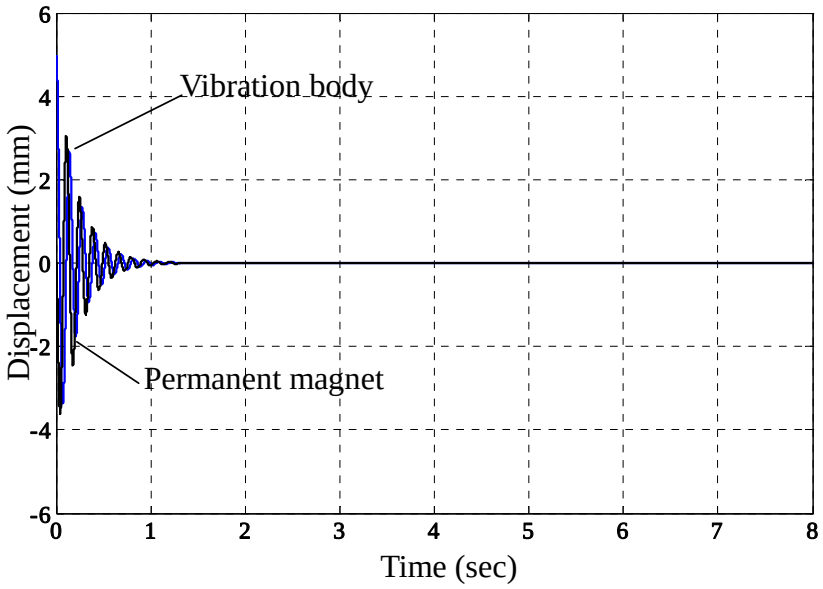

(a)

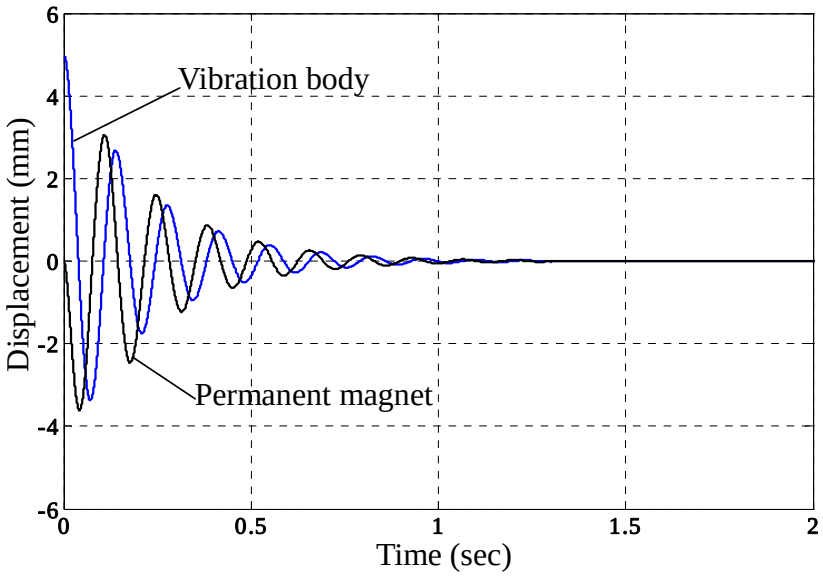

(b)

Fig. 4.4 Simulation result of displacement signal of the vibration body and permanent magnet, the following system conditions: 1) impulse response and 2) with feedback control, gains set to LQR2

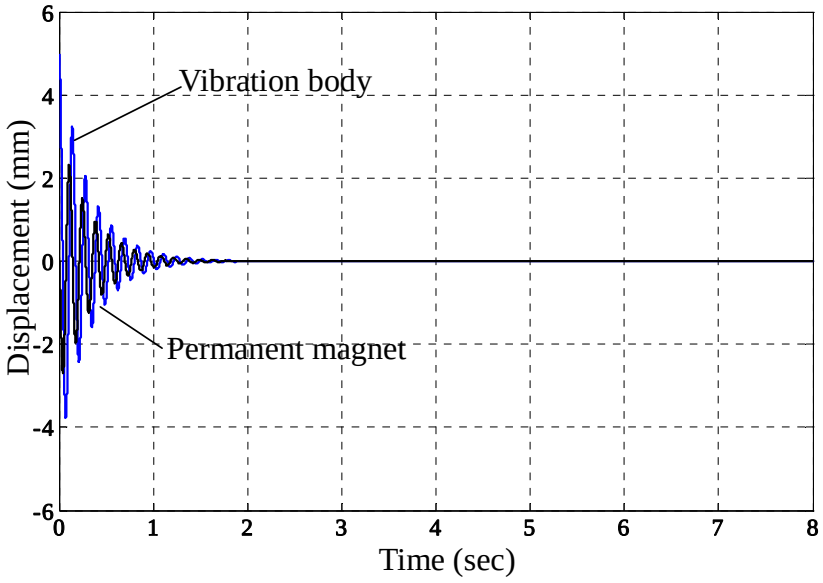

(a)

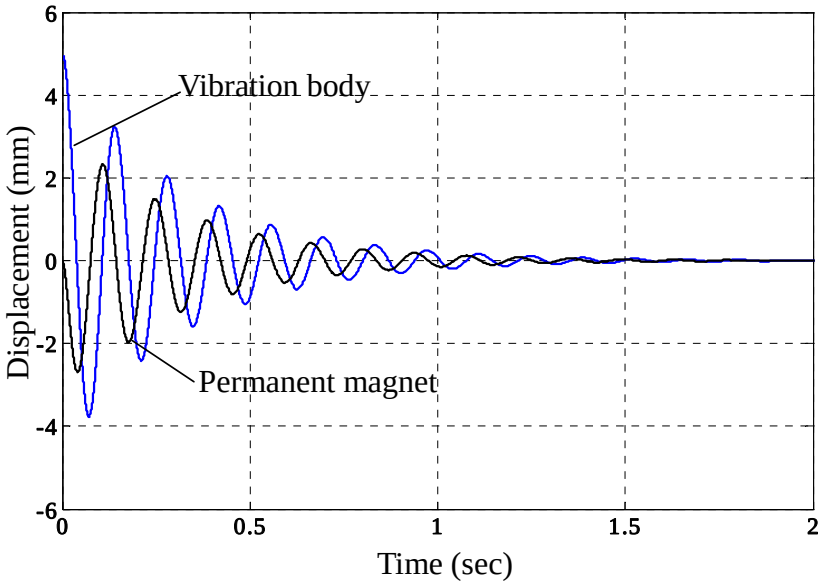

(b)

Fig. 4.5 Simulation result of displacement signal of the vibration body and permanent magnet, the following system conditions: 1) impulse response and 2) with feedback control, gains set to LQR3

Figures 4.3, 4.4 and 4.5 shown the simulation result of the impulse response in case of the feedback controls are set to LQR1, LQR2 and LQR3, respectively. In the figure, figure (a) shown the signal from vibration body and permanent magnet, the transient response of the system is shown in figure (b) where the blue line indicated the displacement signal from vibration body and the black line is indicated the displacement signal from the permanent magnet. As a results, It can be shown that when the system have feedback control the attractive force of permanent magnet acting to vibration body to reach to the equilibrium position sooner than without feedback control as be shown in Fig. 4.2.

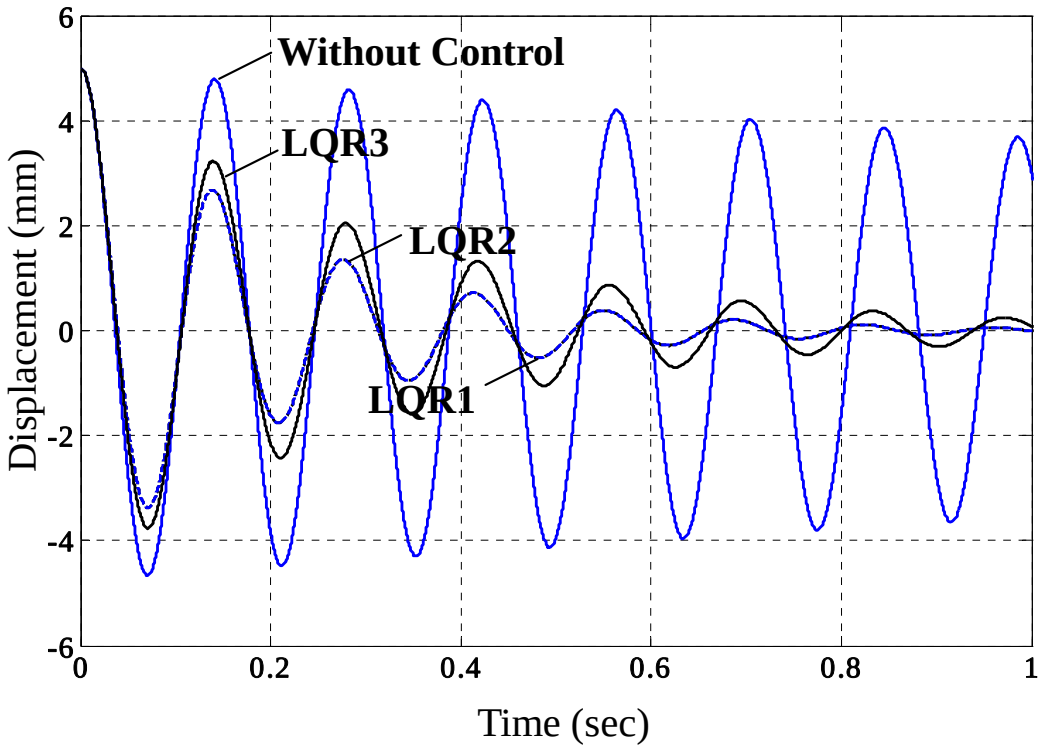

Fig. 4.6 Simulation result of displacement signal of the vibration body, the following system conditions: 1) impulse response, 2) without feedback control, 3) with feedback control, gains set to LQR1, 4) with feedback control, gains set to LQR2 and 5) with feedback control, gains set to LQR3.

Figure 4.6 shows the transient response of vibration body when the feedback controls were without control, with feedback control set to LQR1, LQR2 and with

feedback control set to LQR3. As the results, it can be seen that the system with feedback control that design by means of LQR1 the amplitude of vibration body signal smaller than the system that designed using LQR2 and the feedback gains that designed by means of LQR2 the amplitude of vibration body smaller than LQR3.

Attractive force of permanent magnet has relationship with feedback gain as equation:

$$f_{vcm} = -(k_{PV} z_0 + k_{DV} z_0' + k_{PP} z_p + k_{DP} z_P') \tag{4.13}$$

According to equation (4.13) and the weighting matrix of LQR approach, element (1,1) of weighting Q has effects to displacement of vibration body, element (3,3) of weighting Q has effects to displacement of permanent magnet, respectively. In conclusion of impulse response, LQR methods were successfully in the vibration control system.

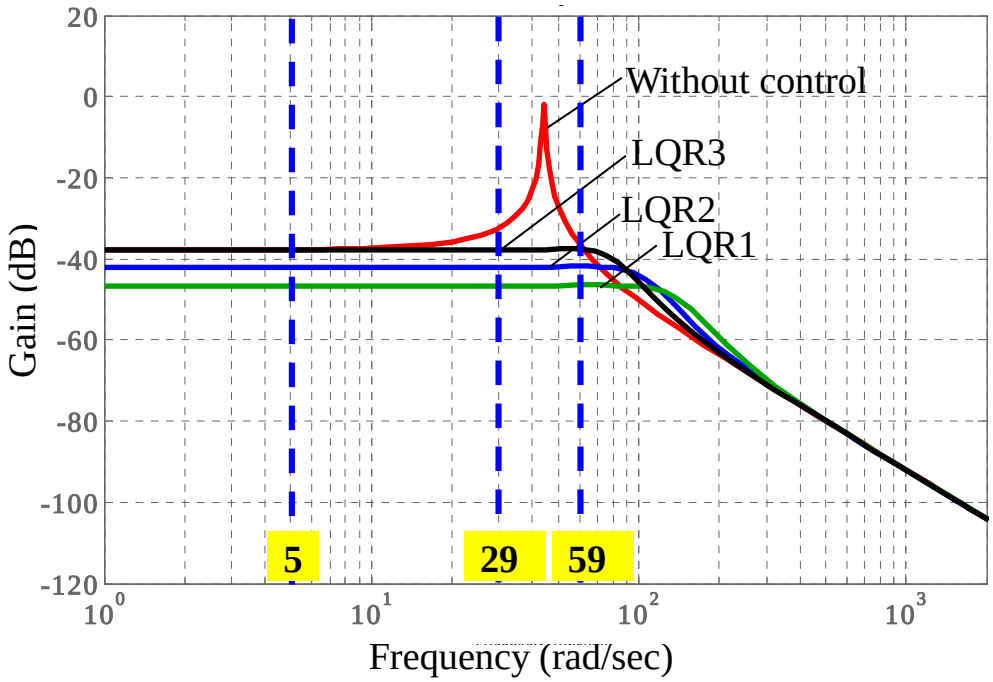

Fig. 4.7 Simulation result of Bode diagram of the displacement signal of the vibration body, the following system conditions: 1) without feedback control, 2) with feedback control, gains set to LQR1, 3) with feedback control, gains set to LQR2 and 4) with feedback control, gains set to LQR3

Figure 4.7 shows simulation result of frequency response, as the results it can be seen that at low frequency the gains of displacement of vibration body to disturbance force were constants, after corner frequency the gains were reduce and at high frequency the gains were lower than high frequency and at the same frequency the gain of LQR1, LQR2 and LQR3 were little difference.

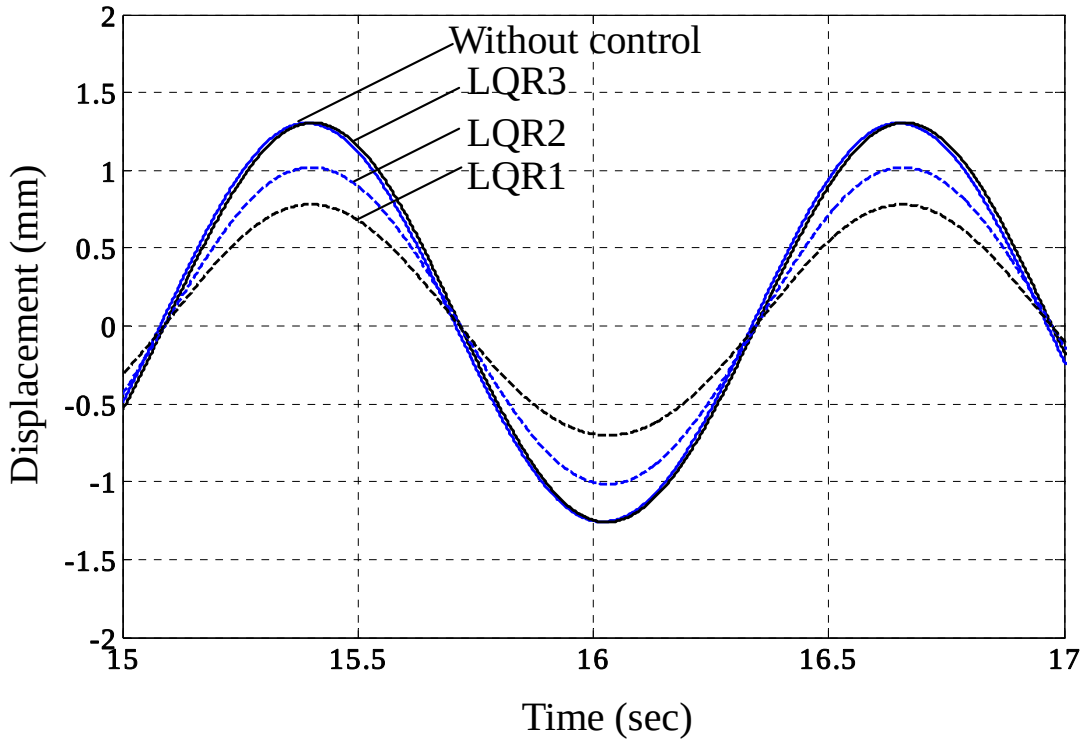

Fig. 4.8 Simulation result of the displacement signal of the vibration body, the following system conditions: 1) disturbance force set to 5 rad/sec, 2)without feedback control, 3) with feedback control, gains set to LQR1, 4) with feedback control, gains set to LQR2 and 5)with feedback control, gains set to LQR3

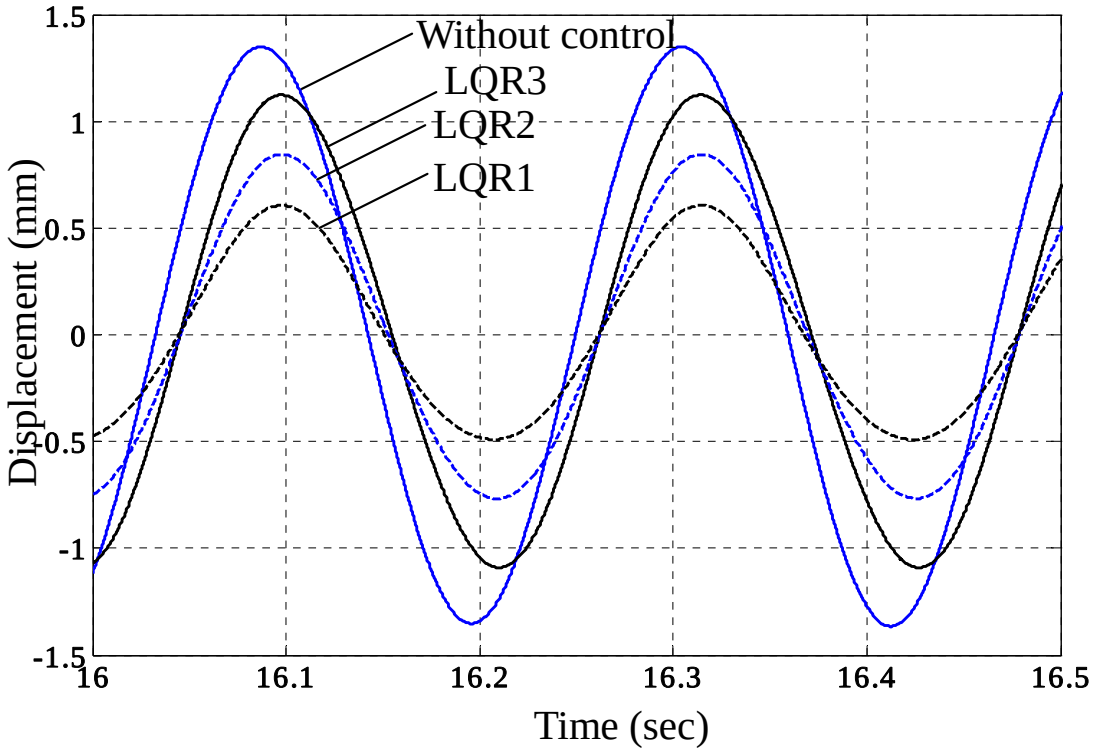

Fig. 4.9 Simulation result of the displacement signal of the vibration body, the following system conditions: 1) disturbance force set to 29 rad/sec, 2)without feedback control, 3) with feedback control, gains set to LQR1, 4) with feedback control, gains set to LQR2 and 5)with feedback control, gains set to LQR3

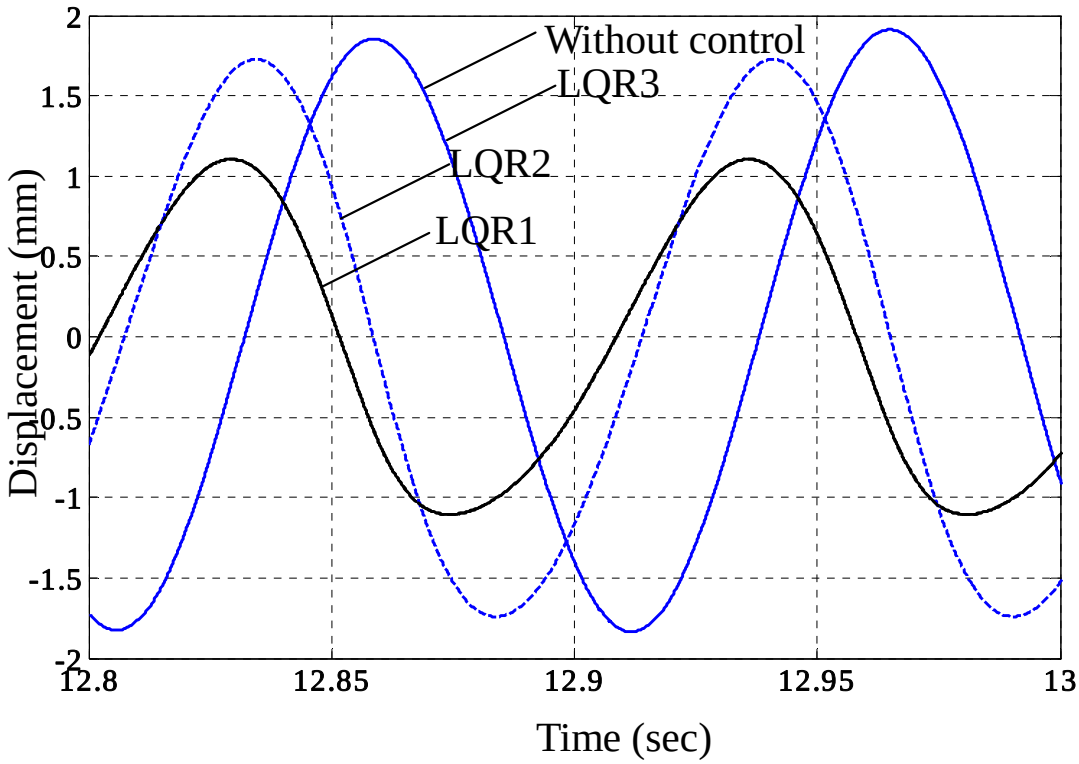

Fig. 4.10 Simulation result of the displacement signal of the vibration body, the following system conditions: 1) disturbance force set to 59 rad/sec, 2)without feedback control, 3) with feedback control, gains set to LQR1, 4) with feedback control, gains set to LQR2 and 5)with feedback control, gains set to LQR3

The frequency responses of the vibration control system are reveal in Fig. 4.8, 4.9 and 4.10, in the figures it can be seen that the feedback control were designed by means of LQR approach were successfully in the vibration control system.

4.4 Experimental Results

Vibration control experiments were also conducted using the experimental prototype shown in Fig. 3.2. Trial under various conditions and equivalent to the numerical simulations were completed.

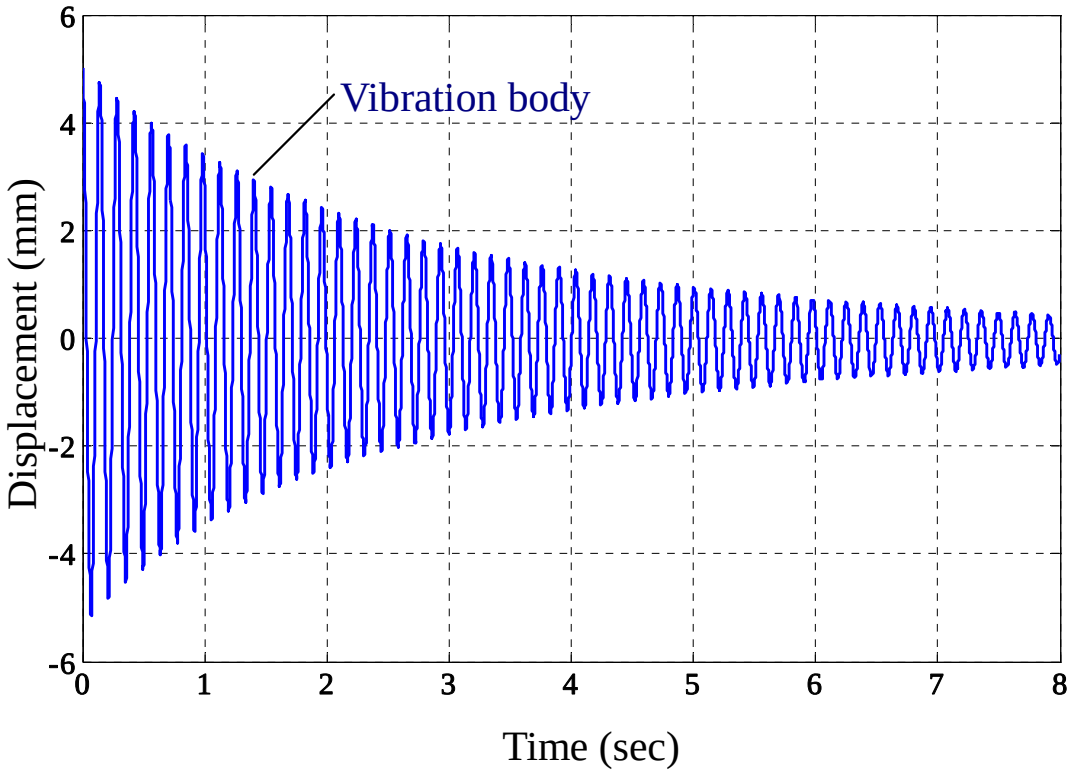

Fig. 4.11 Experimental result of displacement signal of the vibration body, the following system conditions: 1) impulse response, 2) without feedback control and 3) with permanent magnet

Figure 4.11 shows the displacement of vibration body when the system condition without controller. As a result, it can be seen that the system stop vibrate longer than 8 second.

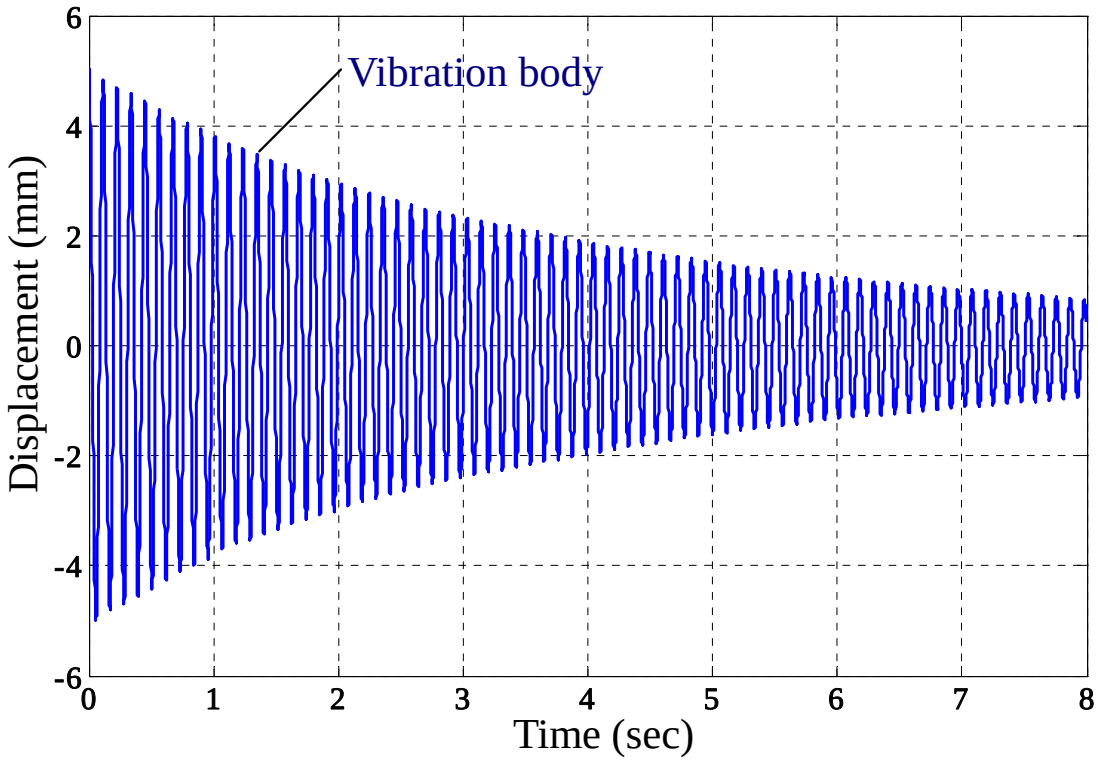

Fig. 4.12 Experimental results of displacement signal of the vibration body, the following system conditions: 1) impulse response, 2) without feedback control and 3) without permanent magnet

Figure 4.12 shows experimental results of the system without feedback control and permanent magnet. Fig 4.11 and 4.12 the equilibrium positions of air-gap are set to 20.00 mm, the vibration amplitude and frequency in Fig. 4.11 are different from those in Fig. 4.12. Therefore, the vibration body will stop vibrate sooner in the system with permanent magnet than in the system without permanent magnet. However, the system will take a longer time to stop vibrating than with feedback control, as shown in Figs. 4.10, 4.11, 4.12 and 4.13.

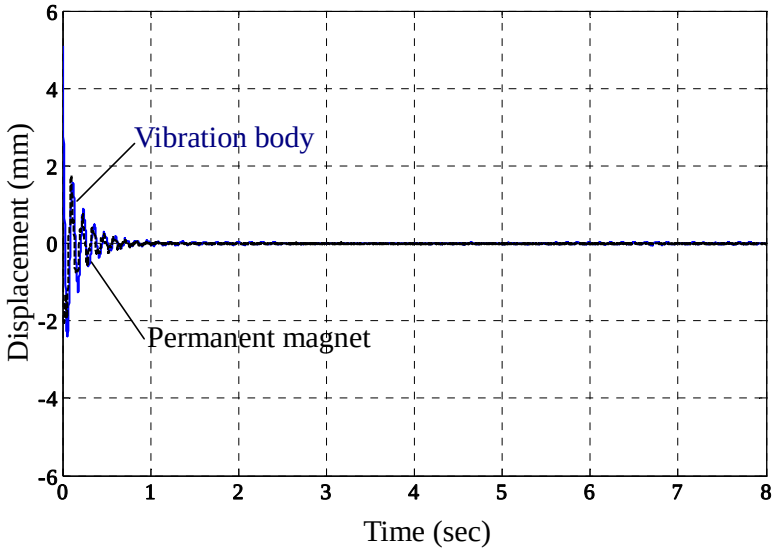

(a)

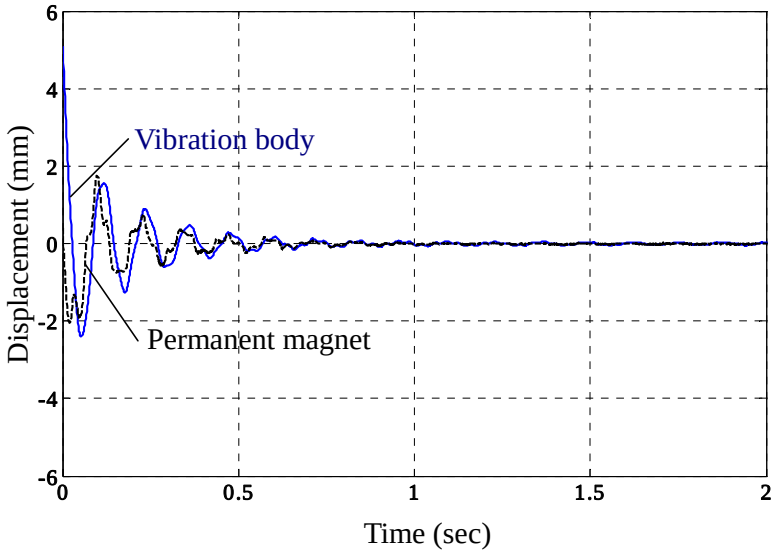

(b)

Fig. 4.13 Experimental result of displacement signal of the vibration body and permanent magnet, the following system conditions: 1) impulse response and 2) with feedback control, gains set to LQR1

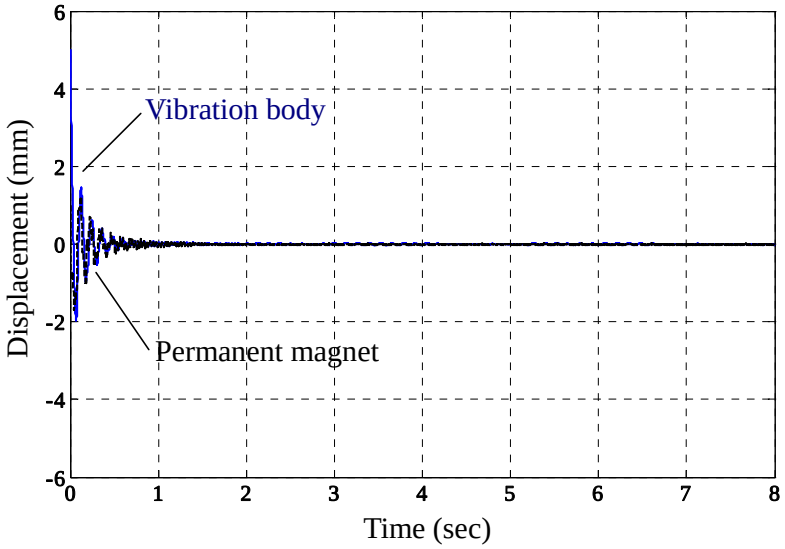

(a)

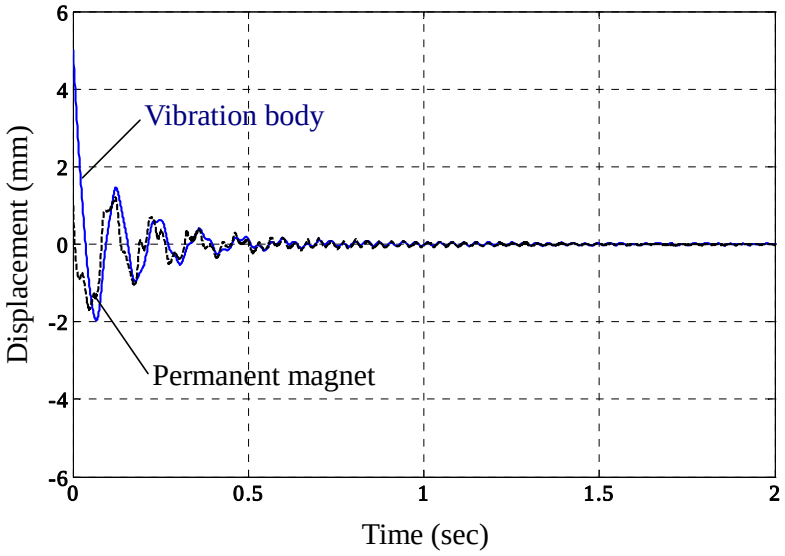

(b)

Fig. 4.14 Experimental result of displacement signal of the vibration body and permanent magnet, the following system conditions: 1) impulse response and 2) with feedback control, gains set to LQR2

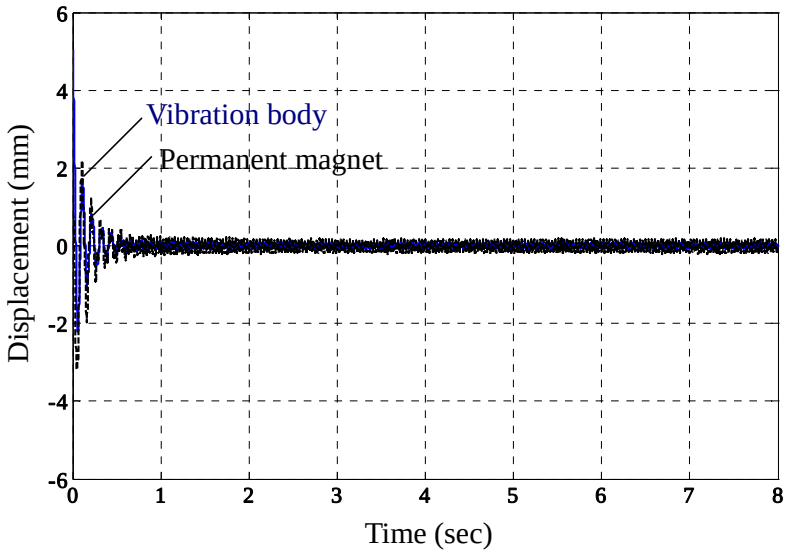

(a)

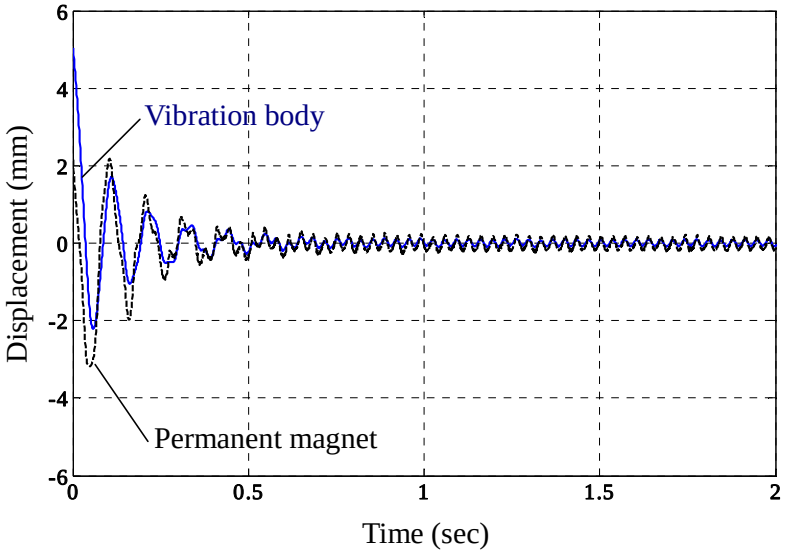

(b)

Fig. 4.15 Experimental results of displacement signal of the vibration body and permanent magnet, the following system conditions: 1) impulse response, 2) with feedback control, gains set to LQR3

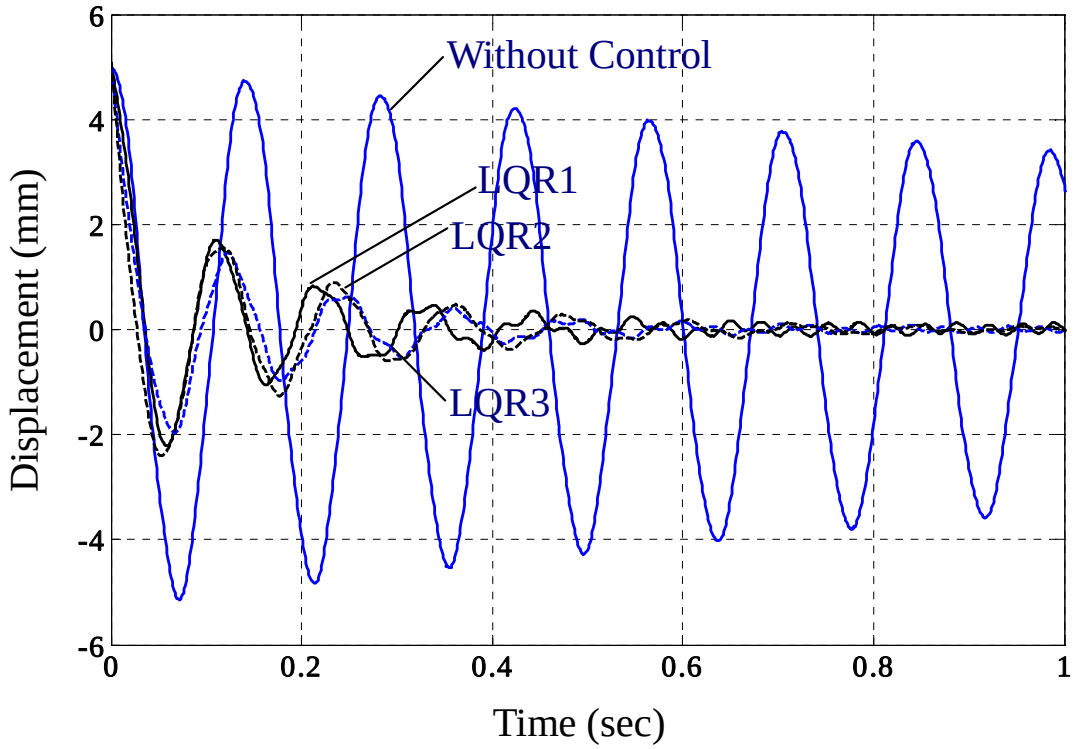

Fig. 4.16 Experimental results of displacement signal of the vibration body, the following system conditions: 1) impulse response, 2) without feedback control, 3) with feedback control, gains set to LQR1 ,4) with feedback control, gains set to LQR2 and 5) with feedback control, gain set to LQR3

Figure 4.13, 4.14, 4.15 and 4.16 are shows the results of feedback control system. The transients response of the system when input is impulse are shows in Figs. 4.13(b), 4.14(b) and 4.15(b). Figure 4.16 shows the transient response in the view point of comparison of feedback controller gain.

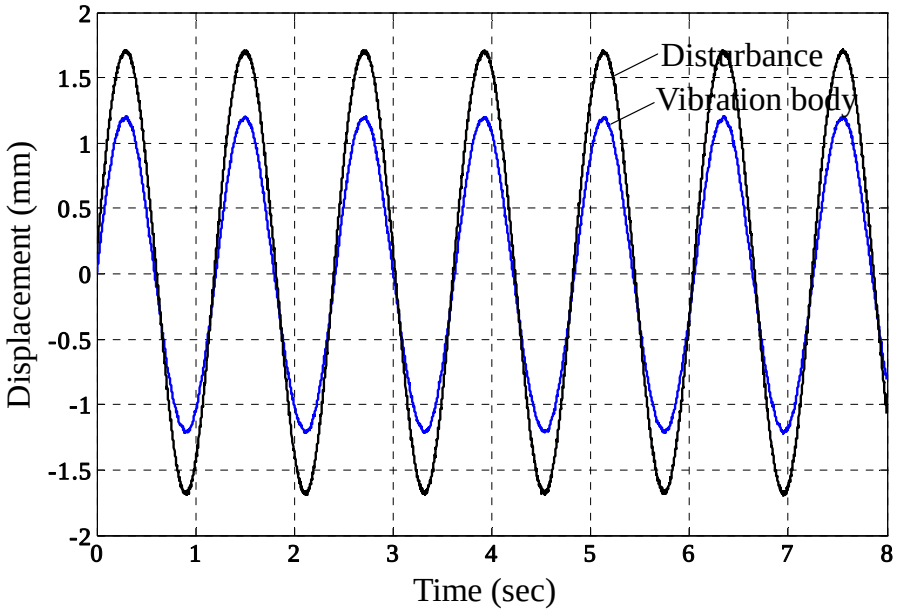

Fig.4.17 Experimental result of displacement signal of the vibration body and signal of the disturbance, the following system conditions: 1) the disturbance frequency set to 5 rad/sec and 2) without feedback control

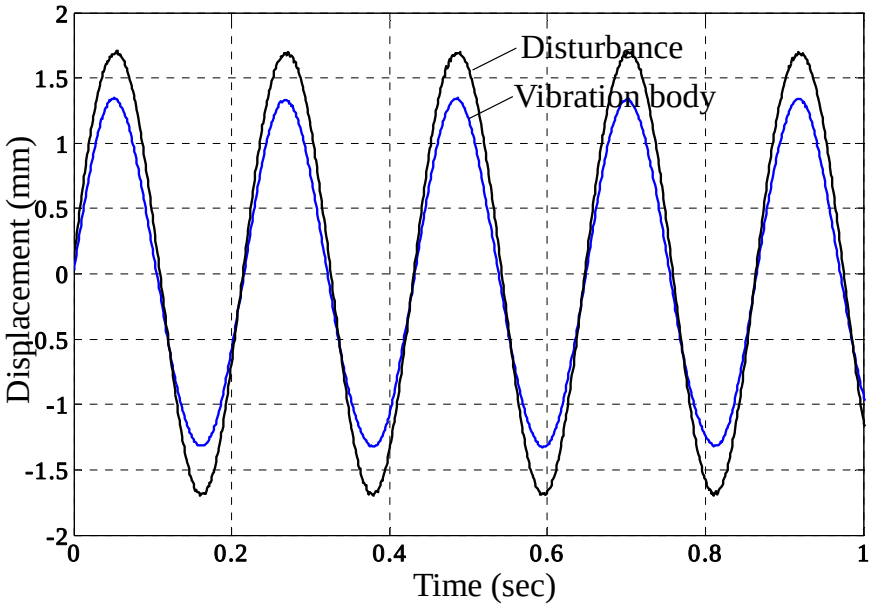

Fig. 4.18 Experimental results of displacement signal of the vibration body and signal of the disturbance, the following system conditions: 1) the disturbance frequency set to 29 rad/sec and 2) without feedback control

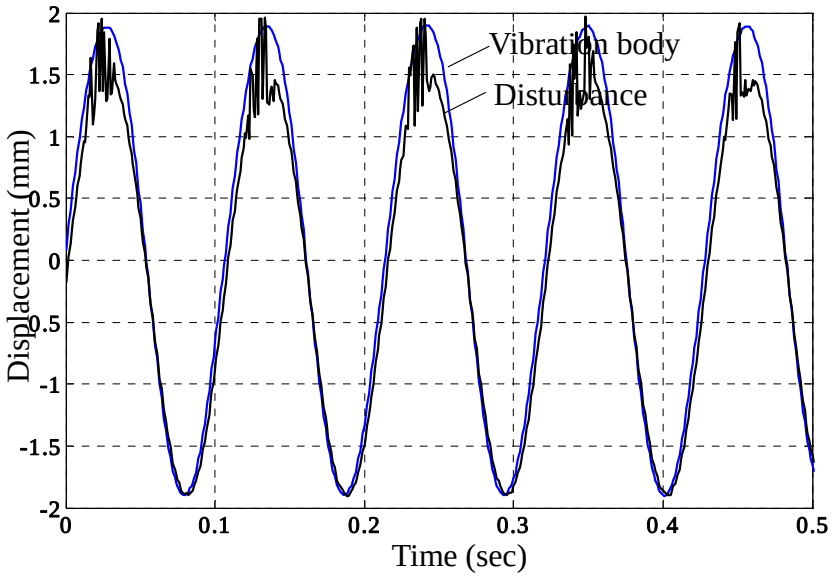

Fig. 4.19 Experimental results of displacement signal of the vibration body and signal of the disturbance, the following system conditions: 1) the disturbance frequency set to 59 rad/sec and 2) without feedback control

Figures 4.17, 4.18 and 4.19 show the displacement of disturbance and vibration body when the frequency of disturbance set to 5, 29 and 59 rad/sec, respectively.

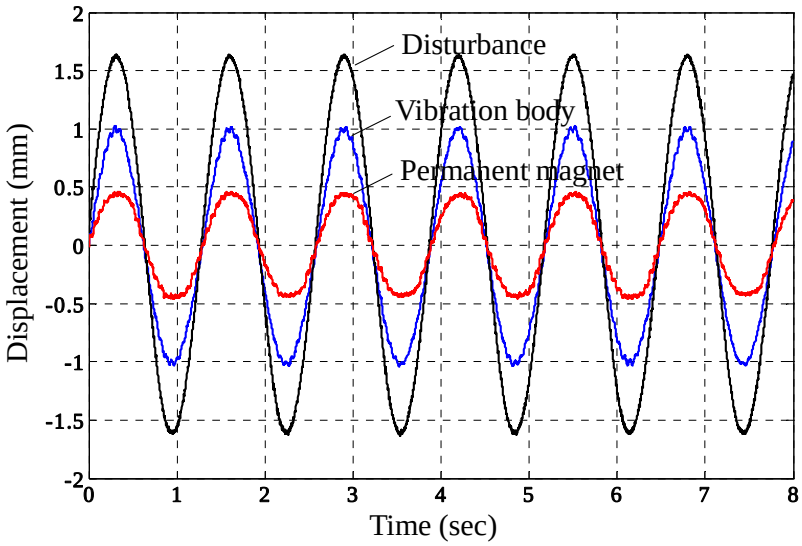

Fig. 4.20 Experimental result of displacement signal of the vibration body, the permanent magnet and the disturbance, the following system conditions: 1) the disturbance frequency set to 5 rad/sec and 2) with feedback control, gains set to LQR1

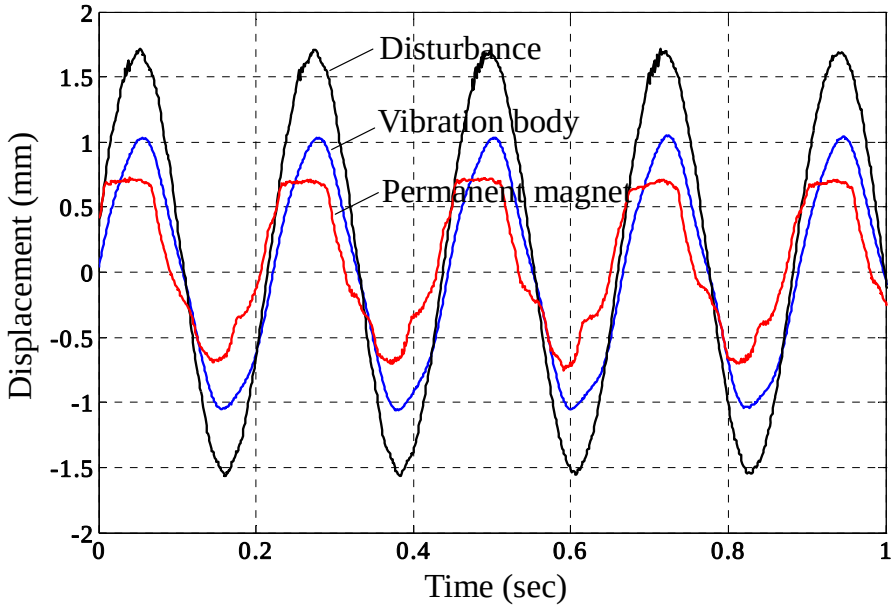

Fig. 4.21 Experimental result of displacement signal of the vibration body, the permanent magnet and the disturbance, the following system conditions: 1) the disturbance frequency set to 29 rad/sec and 2) with feedback control, gains set to LQR1

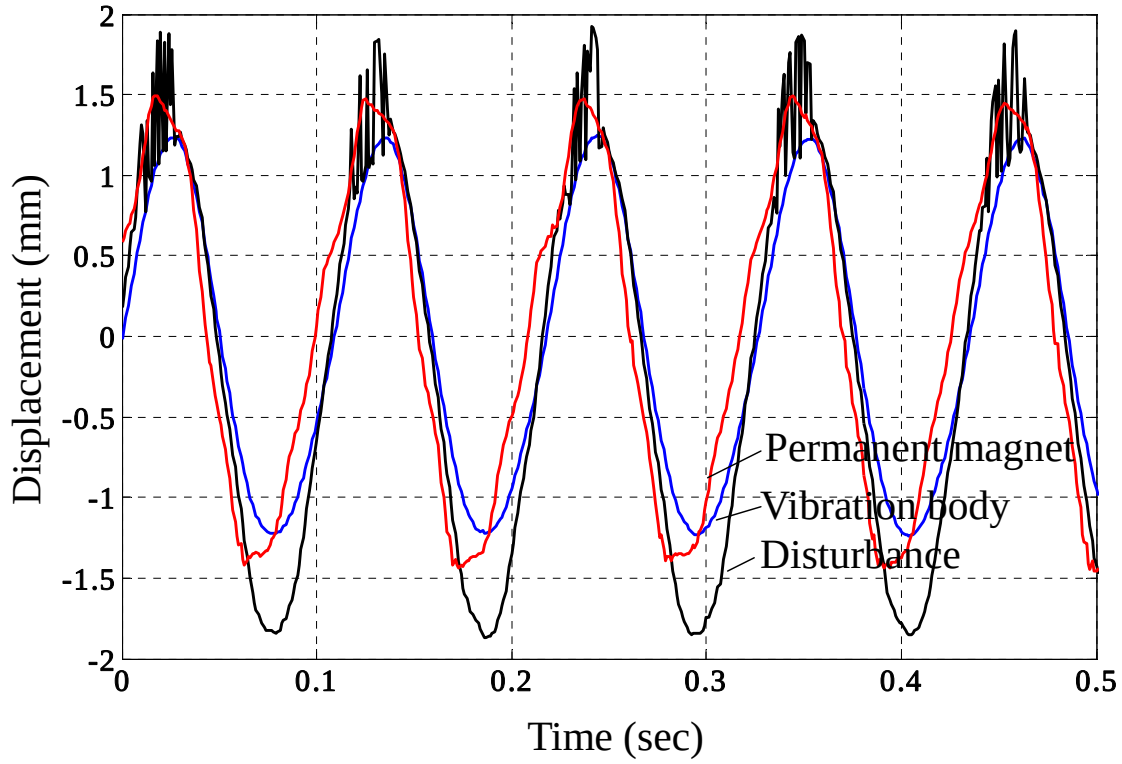

Fig. 4.22 Experimental result of displacement signal of the vibration body, the permanent magnet and the disturbance, the following system conditions: 1) the disturbance frequency set to 59 rad/sec and 2) with feedback control, gains set to LQR1

Figures 4.20, 4.21 and 4.22 show the displacement signal from vibration body, the permanent magnet and the disturbance. The frequencies of disturbance set to 5, 29 and 59 rad/sec, respectively. The feedback control was designed by means of LQR method, the feedback gains set to LQR1. As the results, it can be indicated the attractive force of permanent magnet acted to the vibration body, the amplitude of vibration body when system with feedback control were smaller than without control.

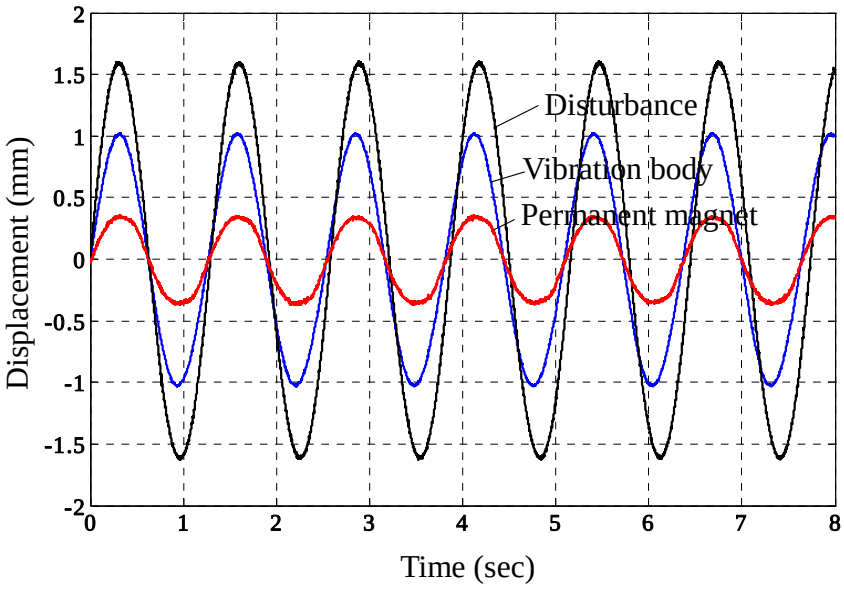

Fig. 4.23 Experimental result of displacement signal of the vibration body, the permanent magnet and the disturbance, the following system conditions: 1) the disturbance frequency set to 5 rad/sec and 2) with feedback control, gains set to LQR2

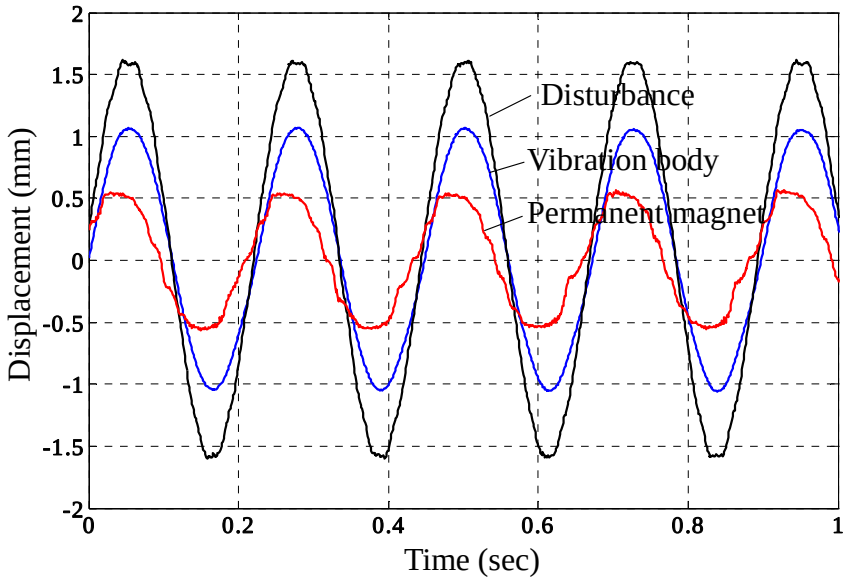

Fig. 4.24 Experimental result of displacement signal of the vibration body, the permanent magnet and the disturbance, the following system conditions: 1) the disturbance frequency set to 29 rad/sec and 2) with feedback control, gains set to LQR2

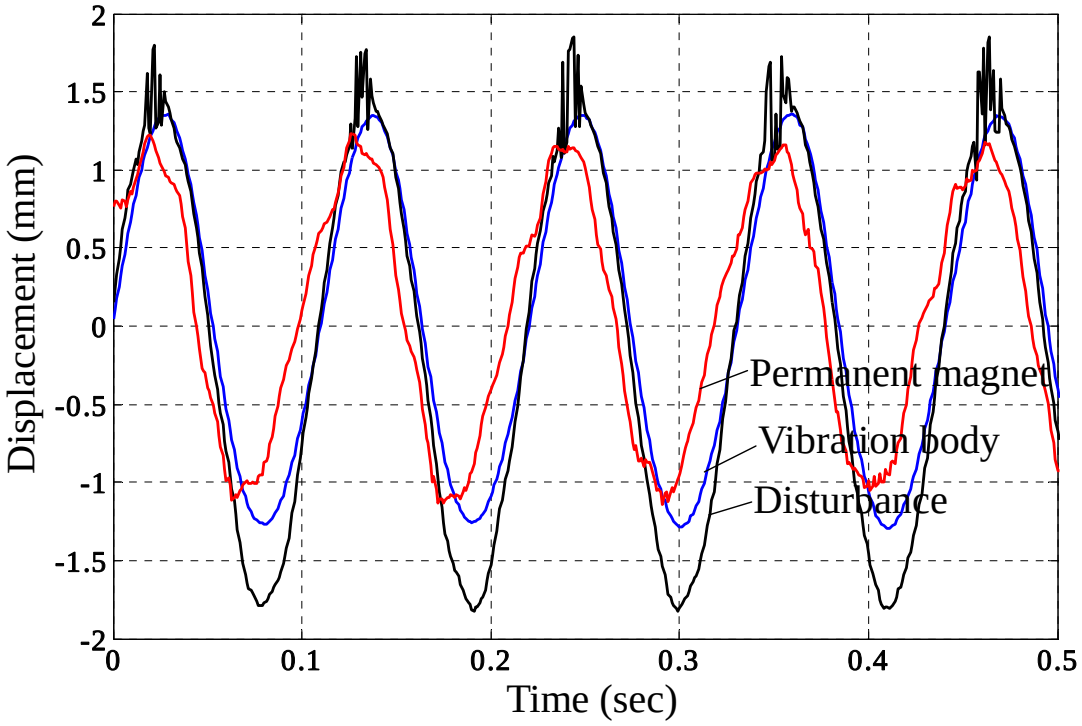

Fig. 4.25 Experimental result of displacement signal of the vibration body, the permanent magnet and the disturbance, the following system conditions: 1) the disturbance frequency set to 59 rad/sec and 2) with feedback control, gain set to LQR2

Figures 4.23, 4.24 and 4.25 show the displacement signal from vibration body, the permanent magnet and the disturbance. The frequencies of disturbance set to 5, 29 and 59 rad/sec, respectively. The feedback control was designed by means of LQR method, the feedback gain set to LQR2. As the results, it can be indicated the attractive force of permanent magnet acted to the vibration body, the amplitude of vibration body when system with feedback control were smaller than without control.

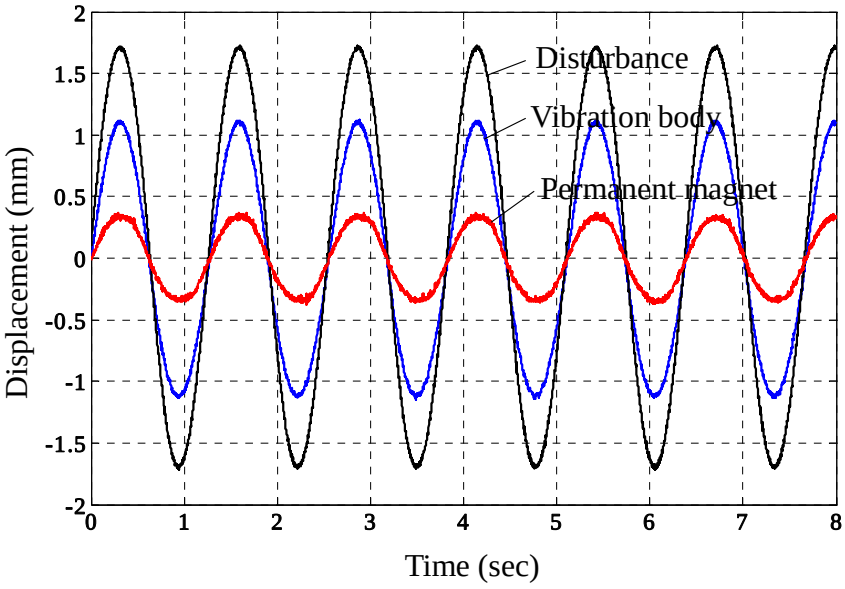

Fig. 4.26 Experimental results of displacement signal of the vibration body, the permanent magnet and the disturbance, the following system conditions: 1) the disturbance frequency set to 5 rad/sec and 2) with feedback control, gains set to LQR3

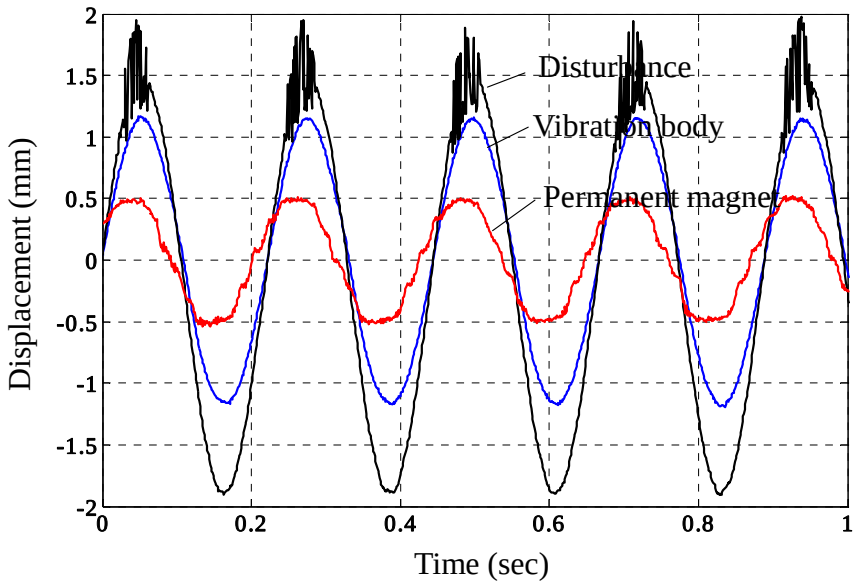

Fig. 4.27 Experimental result of displacement signal of the vibration body, the permanent magnet and the disturbance, the following system conditions: 1) the disturbance frequency set to 29 rad/sec and 2) with feedback control, gains set to LQR3

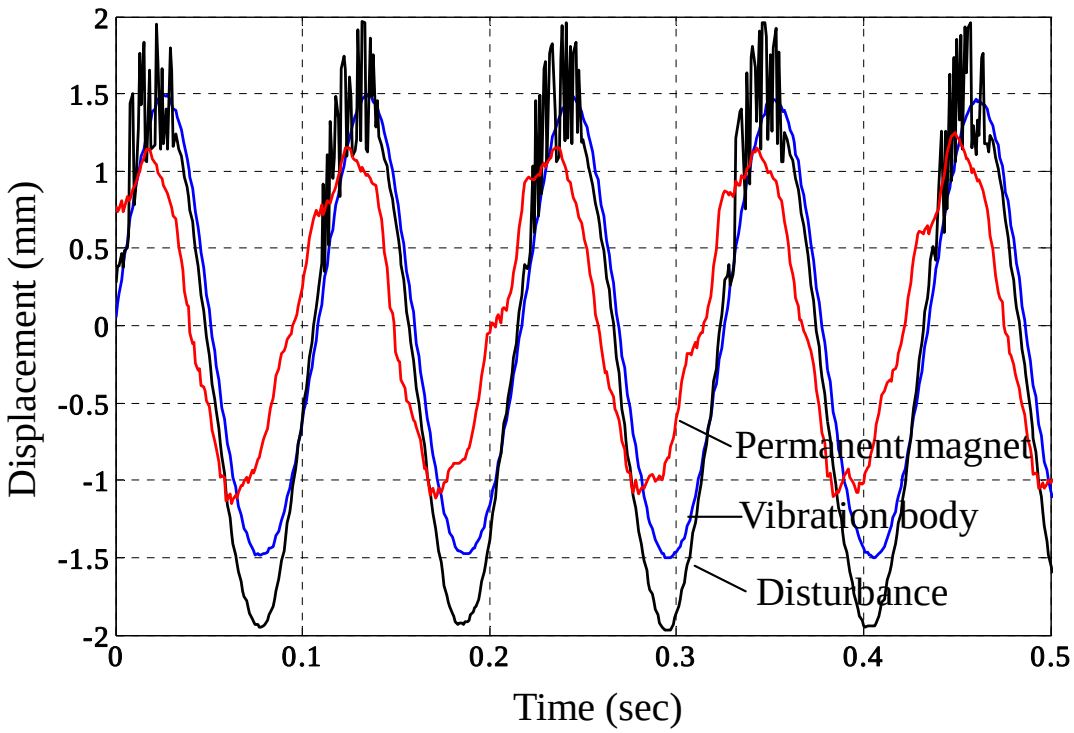

Fig. 4.28 Experimental result of displacement signal of the vibration body, the permanent magnet and the disturbance, the following system conditions: 1) the disturbance frequency set to 59 rad/sec and 2) with feedback control, gains set to LQR3

Figures 4.26, 4.27 and 4.28 show the displacement signal from vibration body, the permanent magnet and the disturbance. The frequencies of disturbance set to 5, 29 and 59 rad/sec, respectively. The feedback control was designed by means of LQR method, the feedback gain set to LQR3. As the results, it can be indicated the attractive force of permanent magnet acted to the vibration body, the amplitude of vibration body when system with feedback control were smaller than without control.

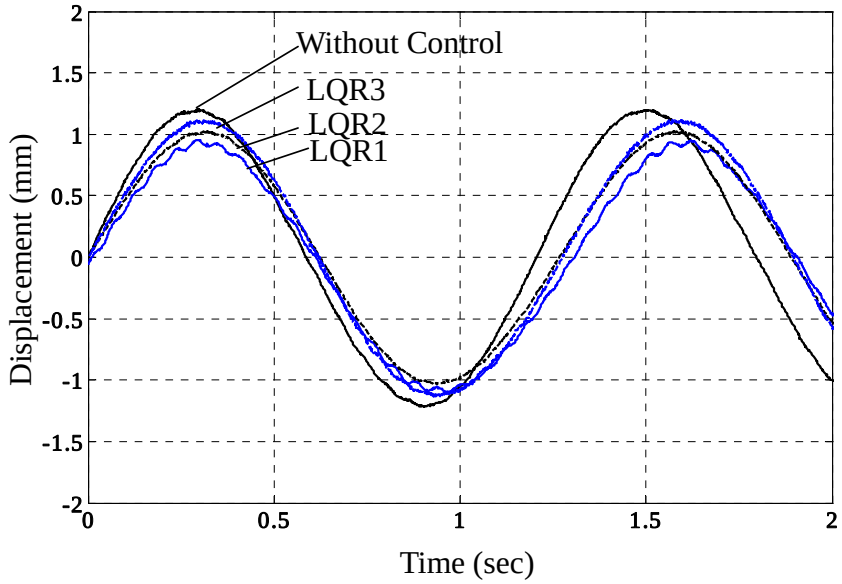

Fig. 4.29 Experimental result of displacement signal of the vibration body, the following system conditions: 1) disturbance frequency set to 5 rad/sec, 2) with feedback control, gains set to LQR1, 3) with feedback control, gains set to LQR2 and 4) with feedback control, gain set to LQR3

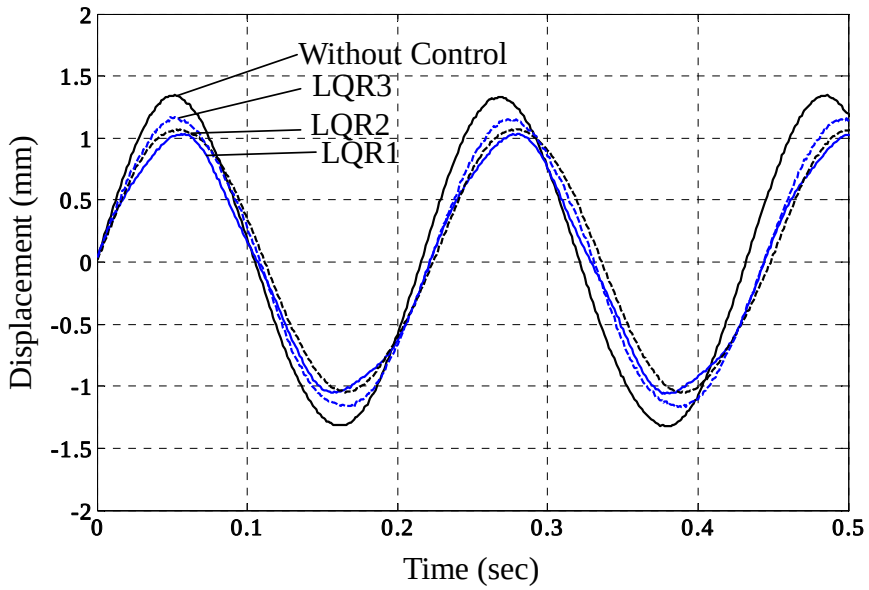

Fig. 4.30 Experimental result of displacement signal of the vibration body, the following system conditions: 1) disturbance frequency set to 29 rad/sec, 2) with feedback control, gain set to LQR1, 3) with feedback control, gain set to LQR2 and 4) with feedback control, gain set to LQR3

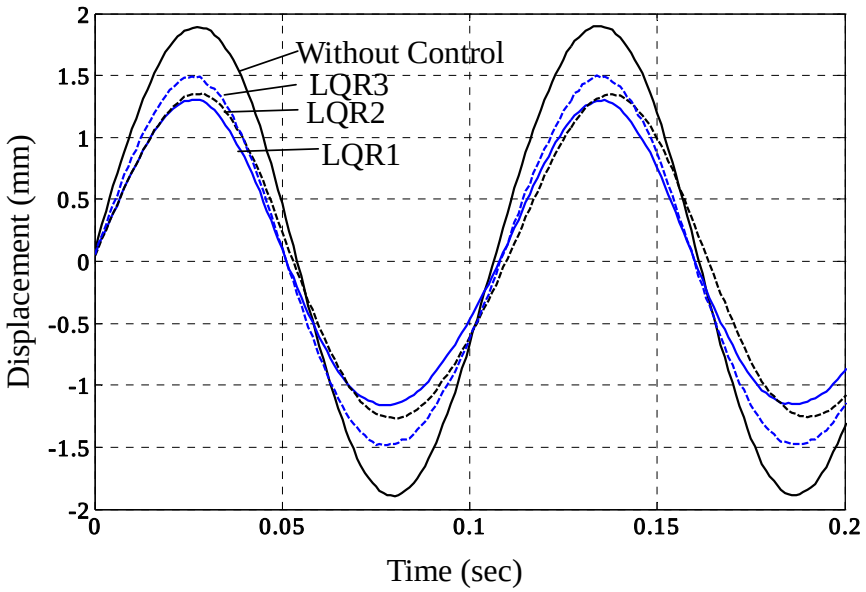

Fig. 4.31 Experimental result of displacement signal of the vibration body, the following system conditions: 1) disturbance frequency set to 59 rad/sec, 2) with feedback control, gains set to LQR1, 3) with feedback control, gains set to LQR2 and 4) with feedback control, gains set to LQR3

Figures 4.29, 4.30 and 4.31 show the comparison of the performance of feedback control in frequency responses. The vibration control system when the feedback control designed using LQR method and vary to LQR1, LQR2 and LQR3, respectively. From the result it can be seen that LQR1 has more effective in frequency response than LQR2 and LQR3.

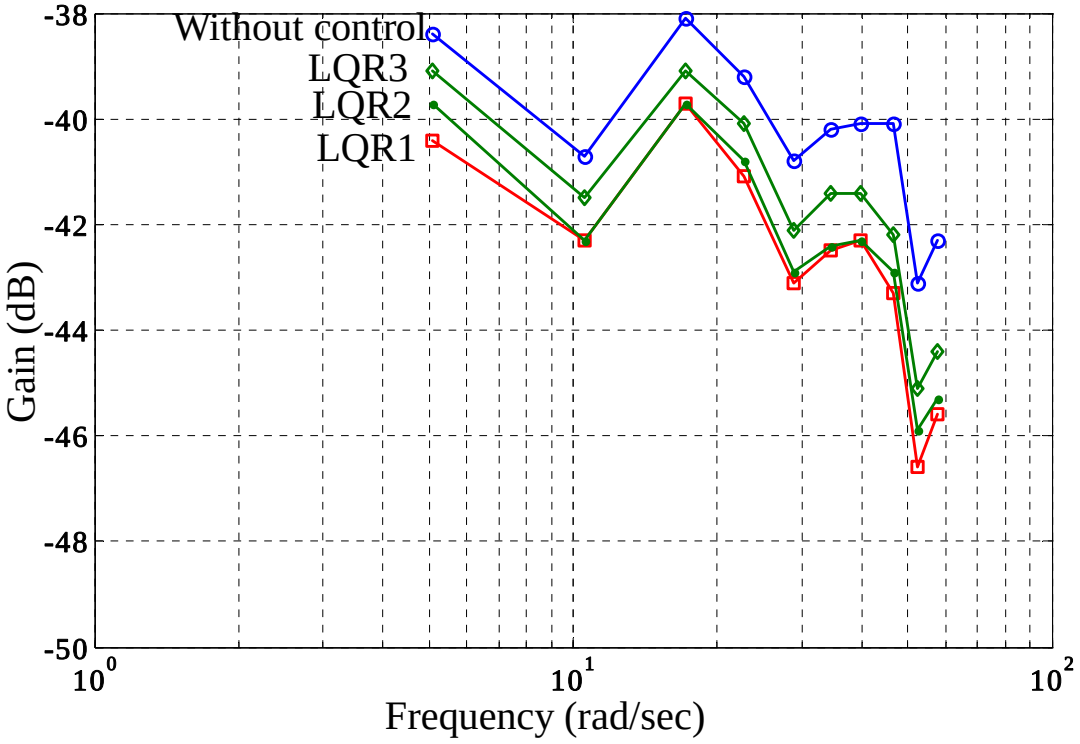

Fig. 4.32 Experimental result of Bode diagram of the displacement signal of the vibration body, the following system conditions: 1) without feedback control, 2) with feedback control, gains set to LQR1, 3) with feedback control, gains set to LQR2 and 4) with feedback control, gains set to LQR3

The frequency response of the vibration control system as shown in Fig. 4.32, in this figure it can be indicated that at the low frequency of disturbance forces, the system has high gain and after corner frequency the system has lower gains than low frequency.

However, when compare with simulation results it can be seen that there have little different because of the different of disturbance force and/or un-control conditions, such as specific and measure value of force, distortion of sinusoidal force, and frequency.

4.5 Conclusions

A vibration suppression control scheme based on linear actuator and permanent magnet is proposed in this chapter. The feedback control was designed using the LQR method. In this chapter, a model was set up for feasibility analysis; the system prototype was manufactured for experimental confirmation.

From the results of simulations and experiments, the following conclusions can be drawn:

- According to the model based on analysis of prototype performance, feedback control was achieved by closed-loop stability.
- Impulse response, the system with feedback controller could suppress the vibration of the object.
- Frequency response, at this view point the system cannot suppress the disturbance force completely, even though the vibration body in case of with feedback controller is lower than in case of the system without feedback controller.

Due to this problem, the feedback control that can suppress in disturbance force is required.

Chapter 5

H_∞ Loop Shaping Approach

5.1 Introduction

This chapter presents the H_∞ Loop Shaping technique using a Loop Shaping Design Procedure (LSDP)[15]-[20]. The LSDP is modern H_∞ optimization approach, suitable for multivariable, robustness and based on concepts from classical Bode plot methods. This chapter begins by the linearized model of vibration control system. The procedure of LSDP approach in vibration control system. Finally, shows the numerical simulation and the experiment results.

5.2 H_∞ Loop Shaping Approach

According to the equation of attractive force of permanent magnet as shown in equation (3.4), by linearization of the attractive force of the magnets, the resultant force can be represented by

$$\tilde{f}_m = k_m(z_v - z_p), \tag{5.1}$$

where k_m is a constant value and equation (3.6) and (3.7) become

$$m_v z_v'' = -k_v z_v - c_v z_v' + k_m(z_v - z_p) + f_d, \tag{5.2}$$

$$m_p z_p'' = -k_p z_p - c_p z_p' + f_{vcm} - k_m(z_v - z_p) \tag{5.3}$$

The system can be represented by the block diagram shown in Fig. 5.1. There are opimal controllers in the loops of the vibration body and the magnets. The feedback gains are calculated by means of H_∞ Loop Shaping technique using a Loop Shaping Design Procedure. Using the LSDP method, a state space model can be derived from Eqs. (3.5),(3.6) and (3.7) as

$$x' = Ax + B_1 u_1 + B_2 u_2 , \tag{5.4}$$

$$y = Cx , \tag{5.5}$$

where

$$A = \begin{bmatrix} 0 & 1 & 0 & 0 \\ \frac{k_m - k_v}{m_v} & -\frac{c_v}{m_v} & -\frac{k_m}{m_v} & 0 \\ 0 & 0 & 0 & 1 \\ -\frac{k_m}{m_p} & 0 & \frac{k_m - k_p}{m_p} & -\frac{c_p}{m_p} \end{bmatrix}$$

$$b_1 = \begin{bmatrix} 0 \\ 0 \\ 0 \\ \frac{1}{m_p} \end{bmatrix}$$

$$b_2 = \begin{bmatrix} 0 \\ \frac{1}{m_v} \\ 0 \\ 0 \end{bmatrix}$$

$u_1 = f_{vcm}$

$u_2 = f_d$

$$y = \begin{bmatrix} z_v \\ z_p \end{bmatrix}$$

$$x = \begin{bmatrix} z_v \\ z_v' \\ z_p \\ z_p' \end{bmatrix} \tag{5.6}$$

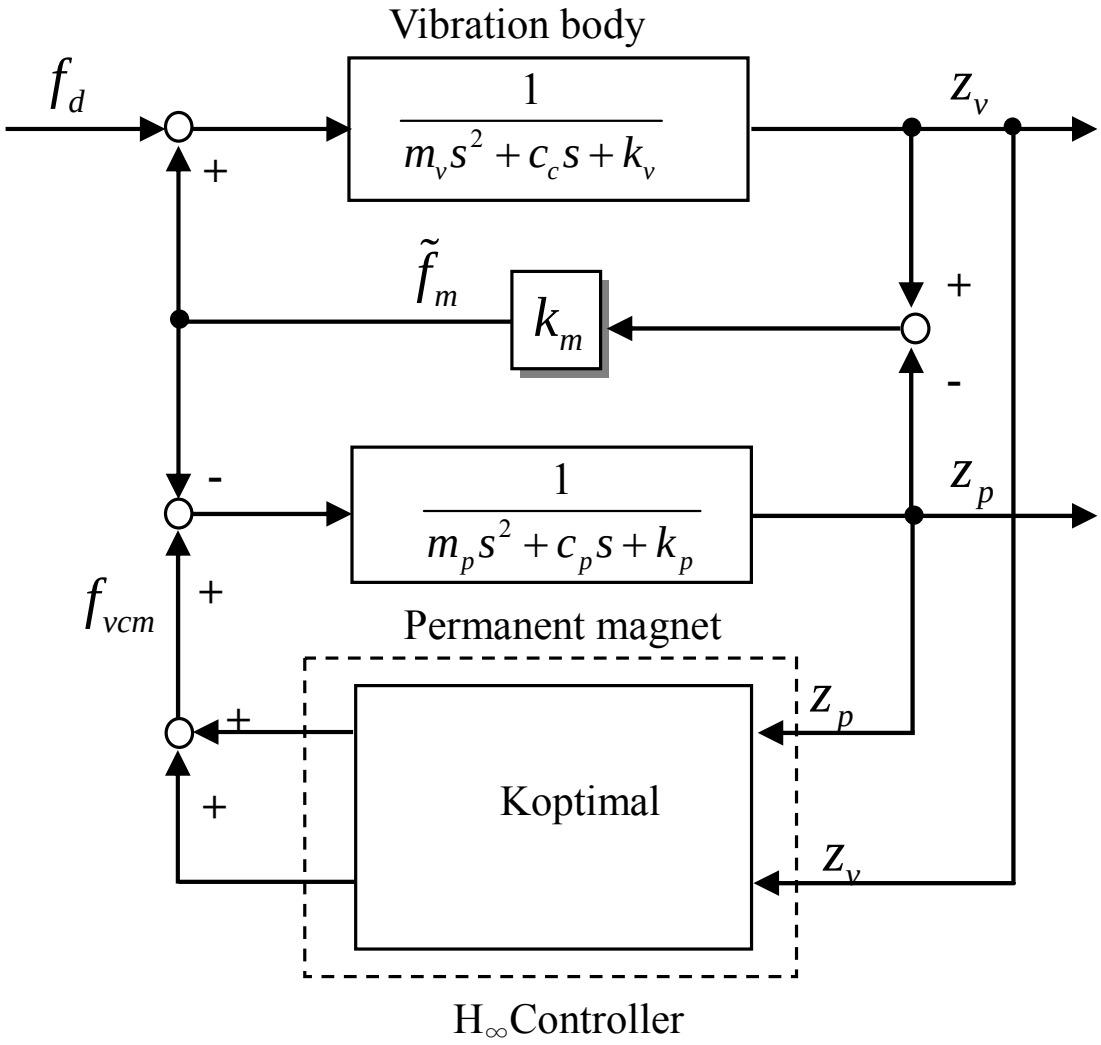

Fig. 5.1 Block-diagram of the vibration control system

The system can be considered as a block diagram shown in Fig. 5.1. There is Feedback controller in the loop of vibration body and the magnets. The optimal feedback gains are calculated by mean of an H_∞ loop shaping design procedure (LSDP), The Glover-McFarlane H_∞ LSDP consists of three steps[25]-[40]:

Step 1) Loop Shaping: In this step, the closed-loop performance is specified in terms of requirements on the open-loop singular values. By using the pre-weighting and post-weighting functions, W_1 and W_2, such that the shaped plat, given by $G_s = W_2 * G * W_1$ has a good shape as shown in Fig.5.2

.

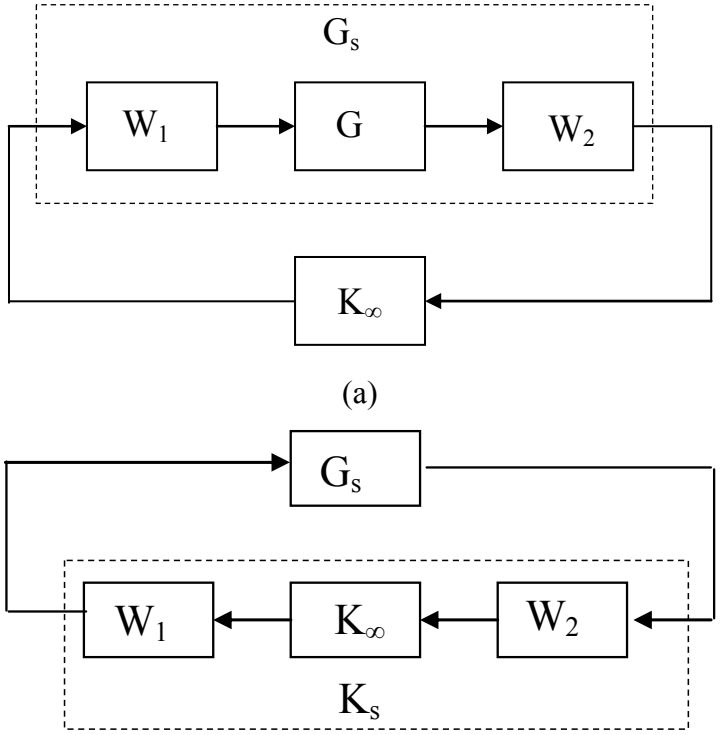

Fig. 5.2 Block diagram of the system

$$W_1 = \frac{831(s+1.376)}{s(s+380)} \tag{5.7}$$

$$W_2 = \begin{bmatrix} 1 & 0 \\ 0 & 1 \end{bmatrix} \tag{5.8}$$

Step 2) Robust Stabilization: Firstly, calculate the maximum stability margin $\varepsilon_{\max}$ as

$$\varepsilon_{\max}^{-1} \triangleq \inf_{K\,stabilizing} \left\| \begin{bmatrix} I \\ K_\infty \end{bmatrix} (I - G_S K_\infty)^{-1} \tilde{M}_S^{-1} \right\|_\infty \tag{5.9}$$

Where $\tilde{M}_S$ and $\tilde{N}_S$ are normalized coprime factors of G_S, $G_S = \tilde{M}_S^{-1}\tilde{N}_S$,

$\tilde{M}_S\tilde{M}_S^T + \tilde{N}_S\tilde{N}_S^T = I$ and $\|.\|_\infty$ denoted to the H_∞ norm. Then synthesis a stabilizing controller K_∞, which satisfies

$$\left\| \begin{bmatrix} I \\ K_\infty \end{bmatrix} (I - G_S K_\infty)^{-1} \tilde{M}_S^{-1} \right\|_\infty \leq \varepsilon^{-1} \tag{5.10}$$

Step 3) Final feedback controller: K_s

The open loop singular value plot of W_1W_2, G and G_s of this system are satisfied and shown in Fig. 5.3.

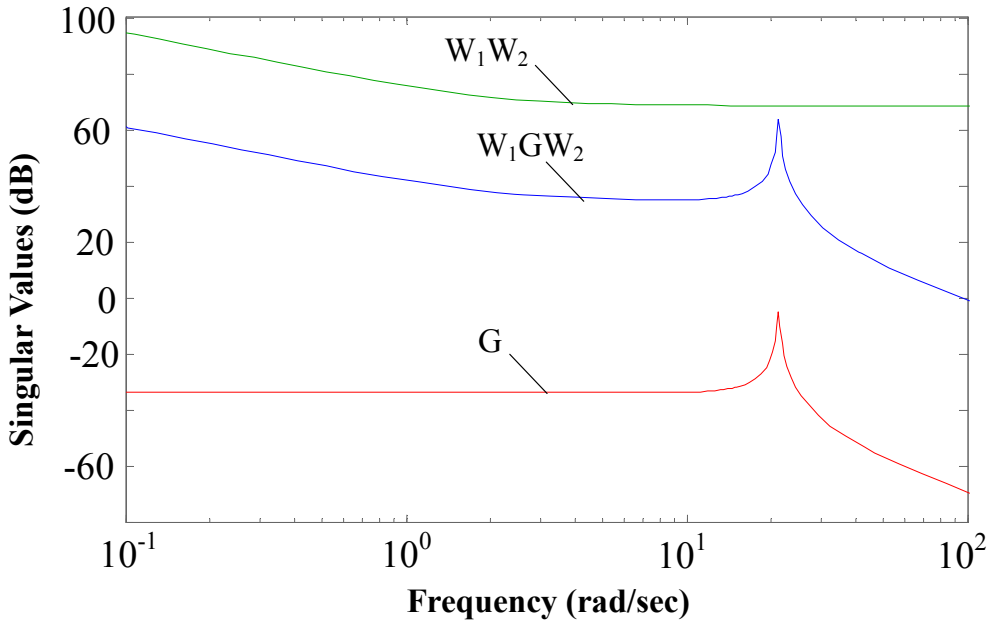

Fig. 5.3 Open-loop singular value plot of W_1W_2, W_1GW_2 and G

5.3 Simulation Results

For feasibility study, numerical simulations carried out with the non-linearization of the attractive force. The simulations are examined in the following cases.

Case 1: impulse response, the system condition are following:

1) without feedback control
2) with feedback control, gain set to LQR1 and
3) with feedback control using H_∞ LSDP

Case 2: frequency response with disturbance force. and the condition are following :

1) without feedback control,
2) with feedback control, gain set to LQR1 and
3) with feedback control using H_∞ LSDP.

The simulations were carried out using the calculated feedback gains in the three cases. In the simulations, the feedback controls in the loop are set to K_1 for LQR.

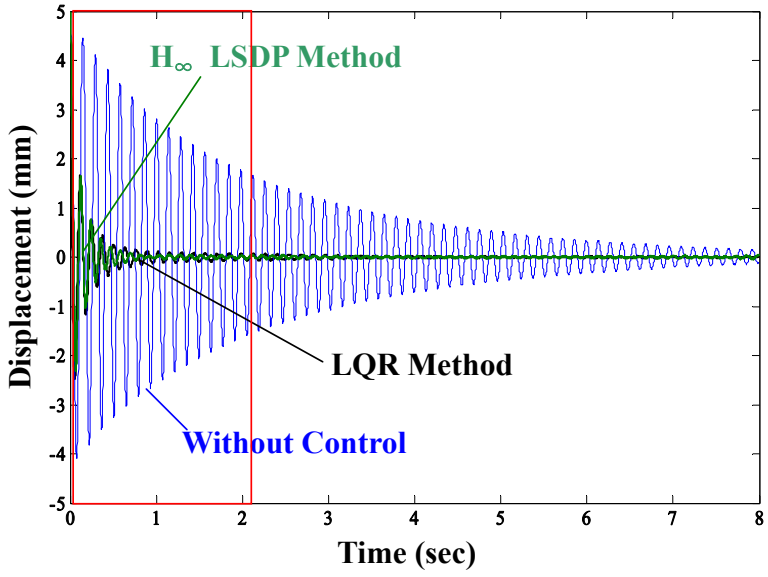

(a)

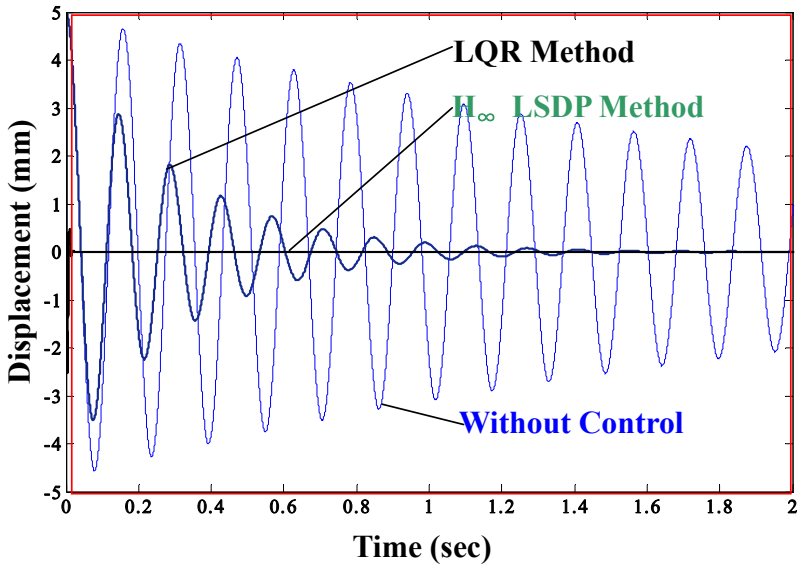

(b)

Fig. 5.4 Simulation result of displacement signal of vibration body, the following system conditions: 1) impulse response, 2) with feedback control, gains set to LQR1 and 3) with feedback control, feedback gains designed using H_∞ LSDP method.

The simulation results in Figs. 5.4 (a) and (b) shows the performance of feedback control. In Fig. 5.4, the equilibrium position of the air-gap is 20 mm. The attractive forces of permanent magnet have changed in order to make the vibration body return to the equilibrium position again. In Fig. 5.4(b) shows the transient response of the simulation results, as can be observed that, in case of with feedback control the vibration body stopped vibrating sooner than that without feedback control.

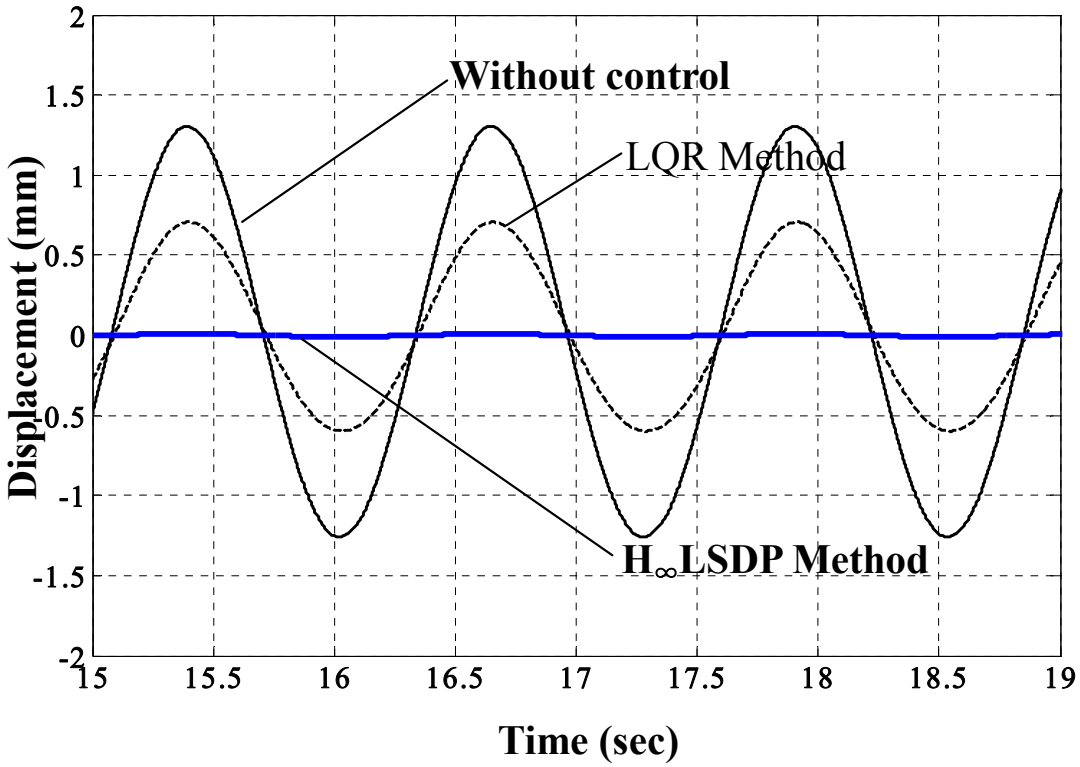

Fig. 5.5 Simulation result of displacement signal of vibration body, the following system conditions: 1) disturbance frequency set to 5 rad/sec, 2)without feedback control, 3) with feedback control, gains set to LQR1 and 4) with feedback control, gains designed using H_∞ LSDP method.

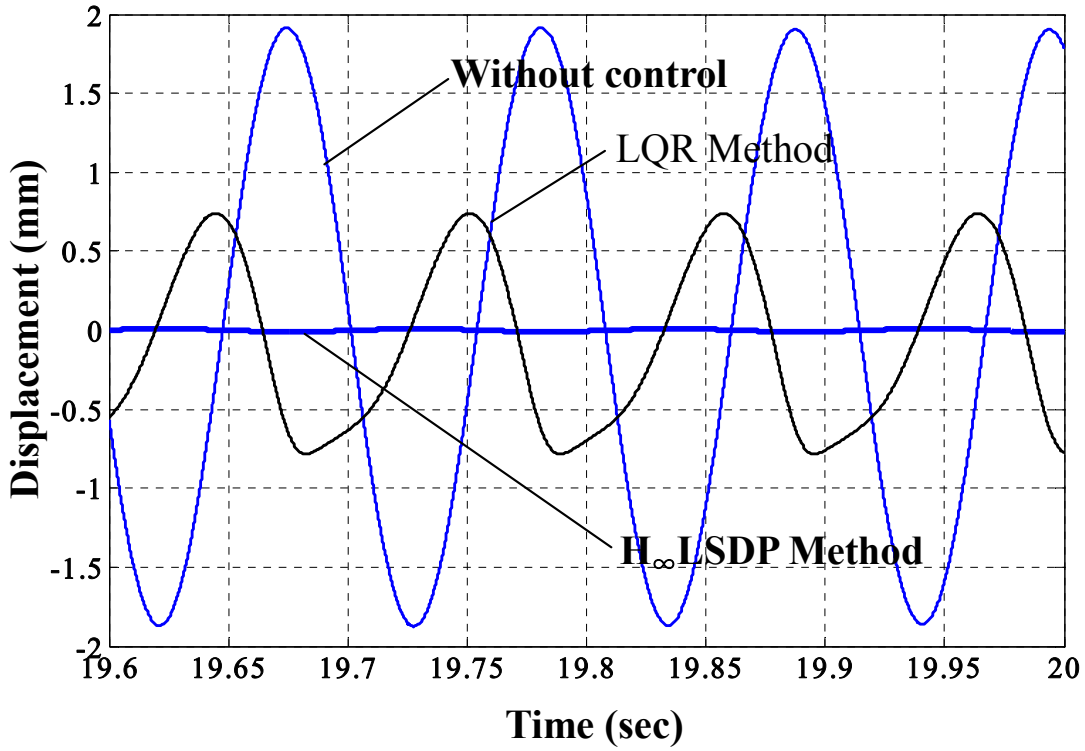

Fig. 5.6 Simulation result of displacement signal of vibration body, the following system conditions: 1) disturbance frequency set to 59 rad/sec, 2)without feedback control, 3) with feedback control, gains set to LQR1 and 4) with feedback control, gains designed using H_∞ LSDP method.

Figure 5.5 and 5.6 shows the frequency responses of vibration control system when the conditions were as follows: 1) with disturbance frequency set to 5 and 59 rad/sec, 2) with feedback control, in the case of feedback control designed using LQR method and gains set to LQR1 and 3) with feedback control, in the case of feedback control designed using H_∞ LSDP method. As the results, it can be observed that the gain of the displacement signal from the vibration body in the system with feedback control is lower than that without feedback control. In addition, the gain of the displacement signal from the vibration body in the system with feedback control was designed using H_∞ LSDP method is lower than the LQR method.

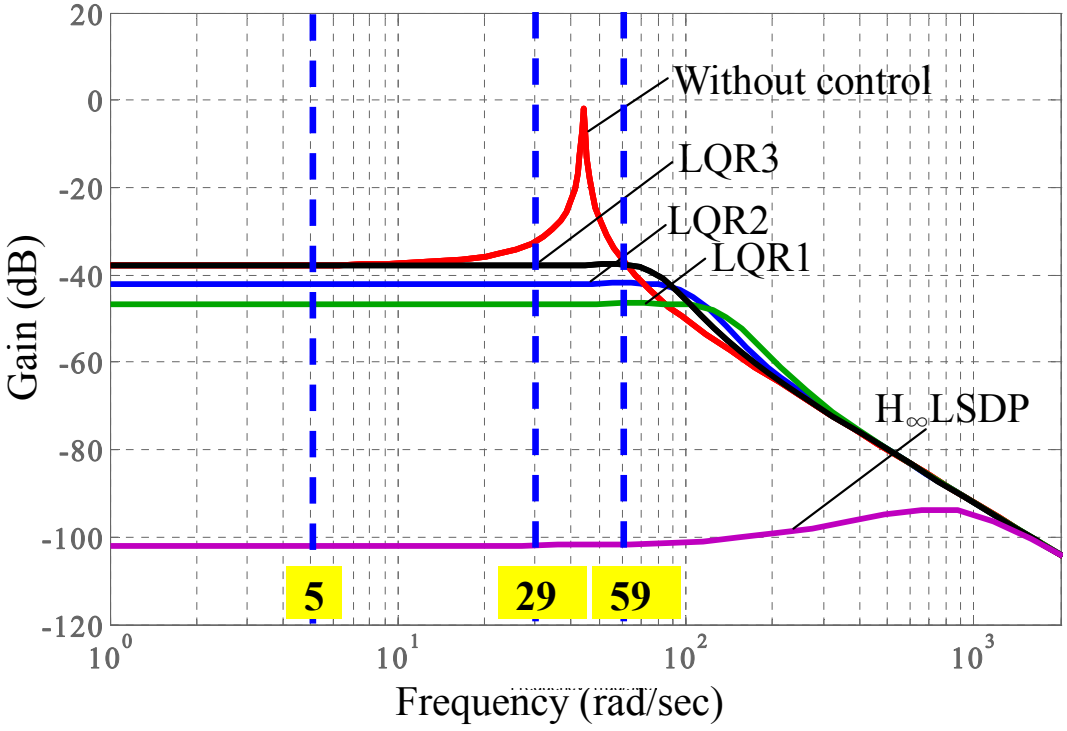

Fig. 5.7 Simulation result of Bode-diagram of the displacement signal from the vibration body and the following system condition 1) without feedback control, 2) with feedback control in case of feedback control designed using LQR method and 3) with feedback control in case of feedback control designed using H_∞ LSDP method.

Figure 5.7 shows the Bode diagram of vibration control system when the conditions were as follows: 1) without feedback control, 2) with feedback control, in the case of feedback control designed using LQR method and 3) with feedback control, in the case of feedback control designed using H_∞ LSDP method. As the results, it can be observed that the gain of the displacement signal from the vibration body in the system with feedback control is lower than that without feedback control. In addition, the gain of the displacement signal from the vibration body in the system with feedback control was designed using H_∞ LSDP method is lower than the LQR method.

5.4 Experimental Results

Vibration control experiments were also conducted using experimental prototype in Fig. 3.2 under both conditions. To study time response and frequency response, trails under 3 conditions:

1) without feedback control,

2) with feedback control, in case of feedback control designed using LQR method and

3) with feedback control, in case of feedback control designed using H_∞ LSDP method.

From the results, impulse response in the case of feedback control was design using the LQR method, with the weighting matrices for calculating the optimal gain set to LQR1 and the feedback gains designed using H_∞LSDP method as shown in Figs. 5.8 and 5.9.

For frequency responses the frequency of the disturbance were set to 5, 29 and 59 rad/sec as shown in Figs. 5.10 to 5.15. The Bode diagram of the vibration control systems and the gains designed using H_∞LSDP method as shown in Fig. 5.16.

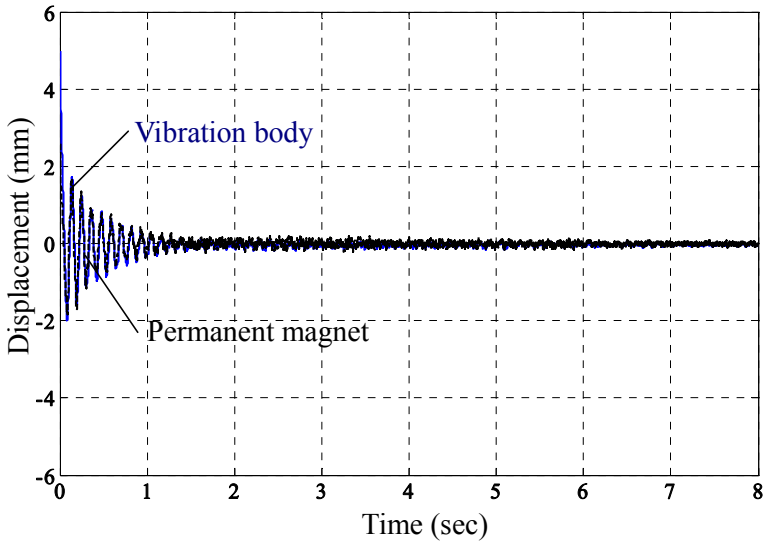

(a)

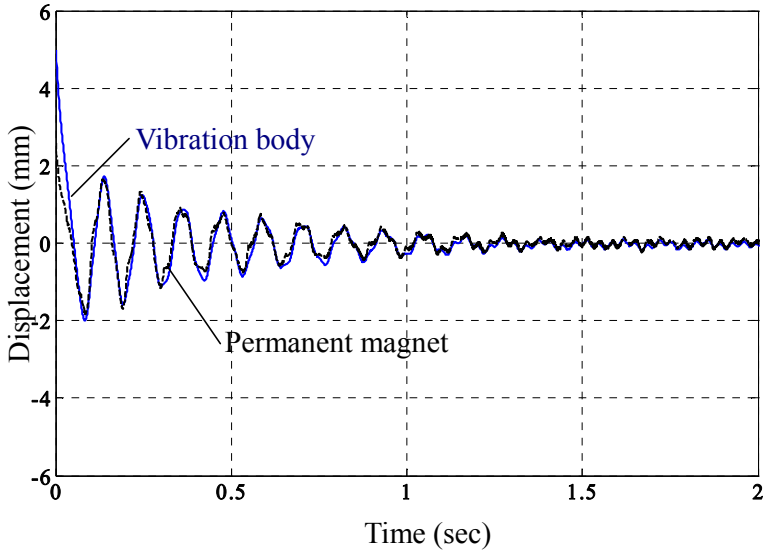

(b)

Fig. 5.8 Experimental results of displacement signal of the vibration body and permanent magnet, the following system conditions: 1) impulse response, 2) with feedback control, designed using H_∞LSDP Method

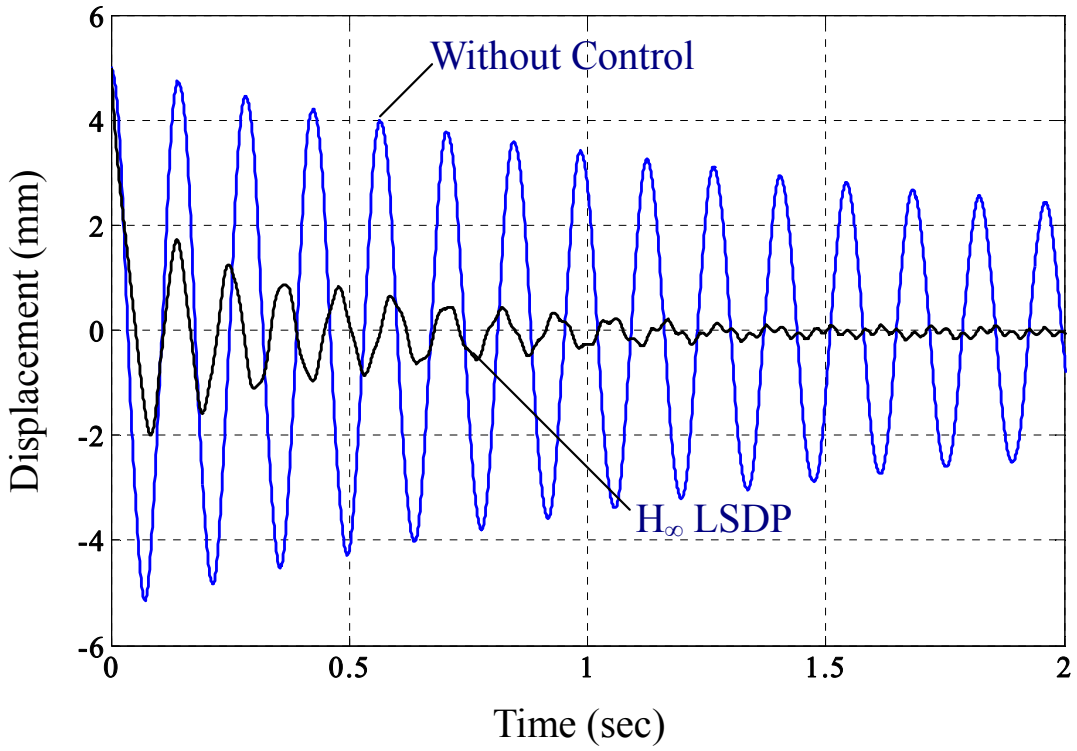

26

Fig. 5.9 Experimental result of displacement signal of the vibration body, the following system conditions: 1) impulse response 2) without feedback control and 3) with feedback control, designed using H_∞LSDP method

Figures 5.6 and 5.7 which show the impulse response of the vibration control system. Fig. 5.6 (b) shows the transient response of the system, as the results it can be seen that the feedback control that designed by means of H_∞LSDP method can be applied to the system.

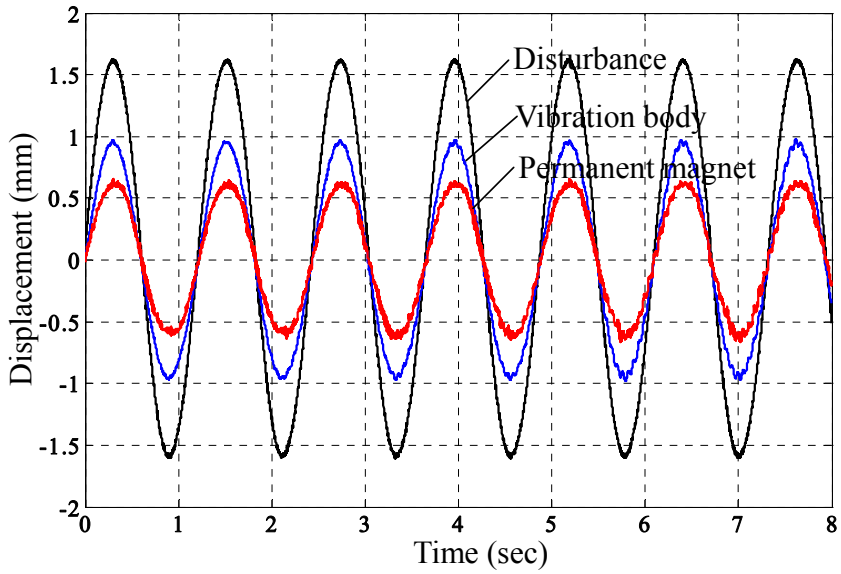

Fig. 5.10 Experimental result of displacement signal of the vibration body, the permanent magnet and the disturbance, the following system conditions: 1) the disturbance frequency set to 5 rad/sec and 2) with feedback control, designed using H_∞LSDP method

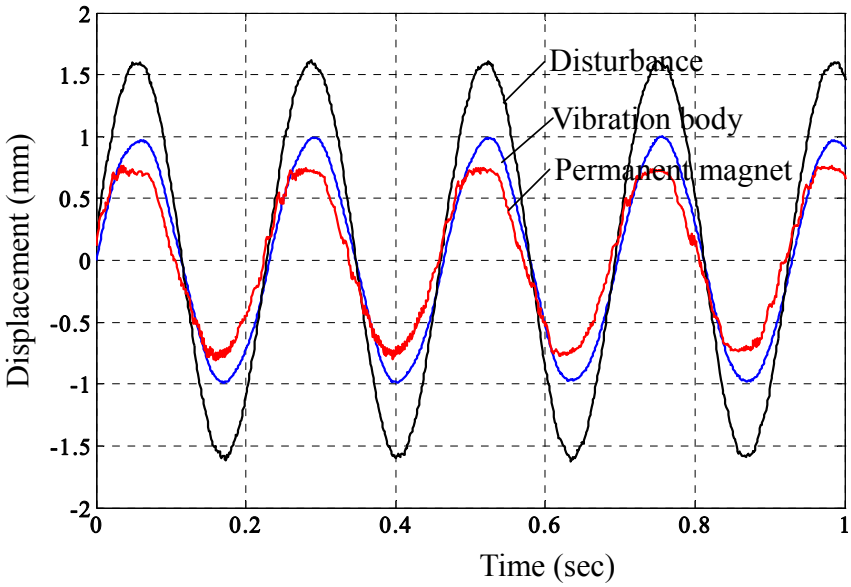

Fig. 5.11 Experimental result of displacement signal of the vibration body, the permanent magnet and the disturbance, the following system conditions: 1) the disturbance frequency set to 29 rad/sec and 2) with feedback control, designed using H_∞LSDP medhod

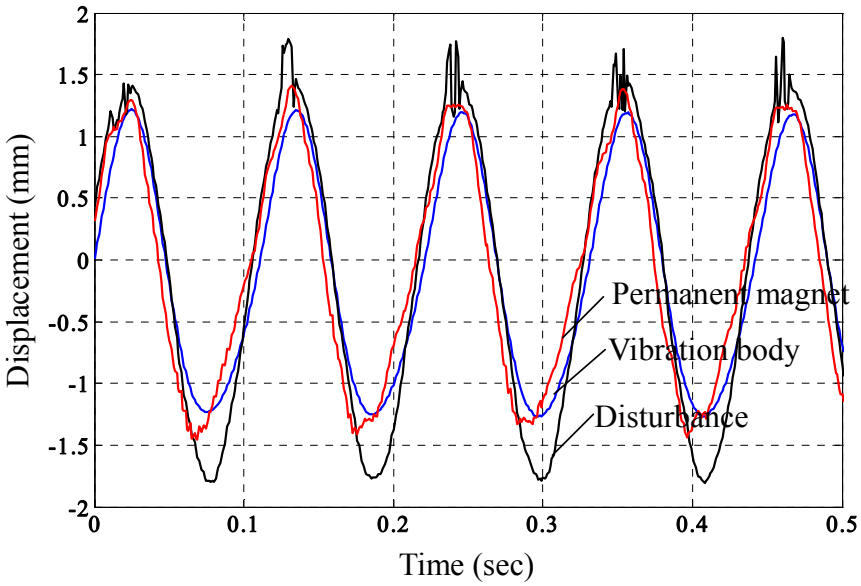

Fig. 5.12 Experimental result of displacement signal of the vibration body, the permanent magnet and the disturbance, the following system conditions: 1) the disturbance frequency set to 59 rad/sec and 2) with feedback control, designed using H_∞LSDP method

Figures 5.0, 5.11 and 5.12 revealed the experimental results for disturbance frequency of 5, 29 and 59 rad/sec. The feedback control designed using the H_∞ LSDP method.

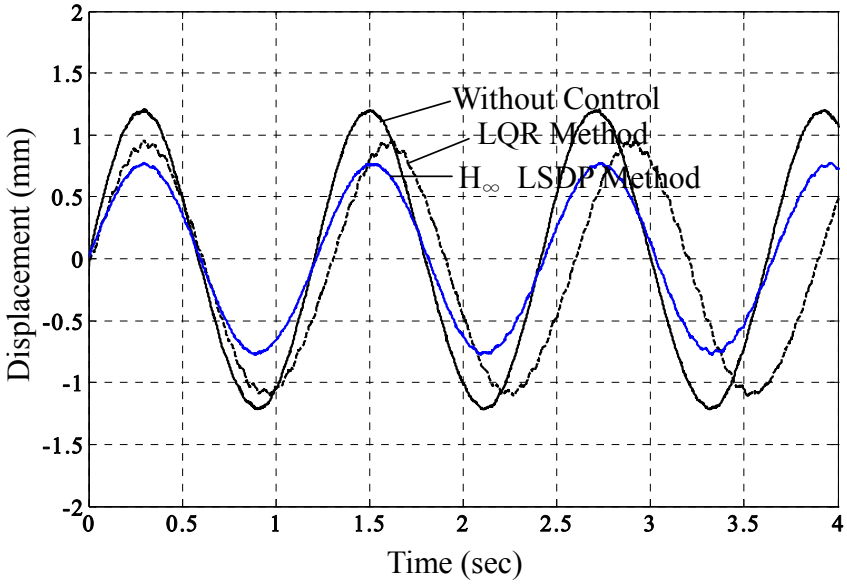

Fig. 5.13 Experimental result of displacement signal of the vibration body, the following system conditions: 1) disturbance frequency set to 5 rad/sec, 2) with feedback control, designed using LQR Method and 3) with feedback control, designed using H_∞LSDP Method

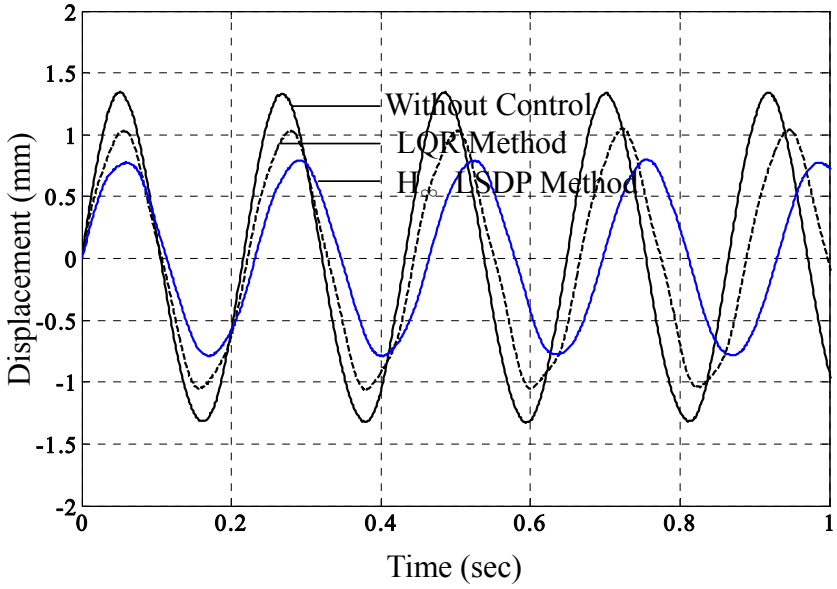

Fig. 5.14 Experimental result of displacement signal of the vibration body, the following system conditions: 1) disturbance frequency set to 29 rad/sec, 2) with feedback control, designed using LQR Method and 3) with feedback control, designed using H_∞LSDP Method

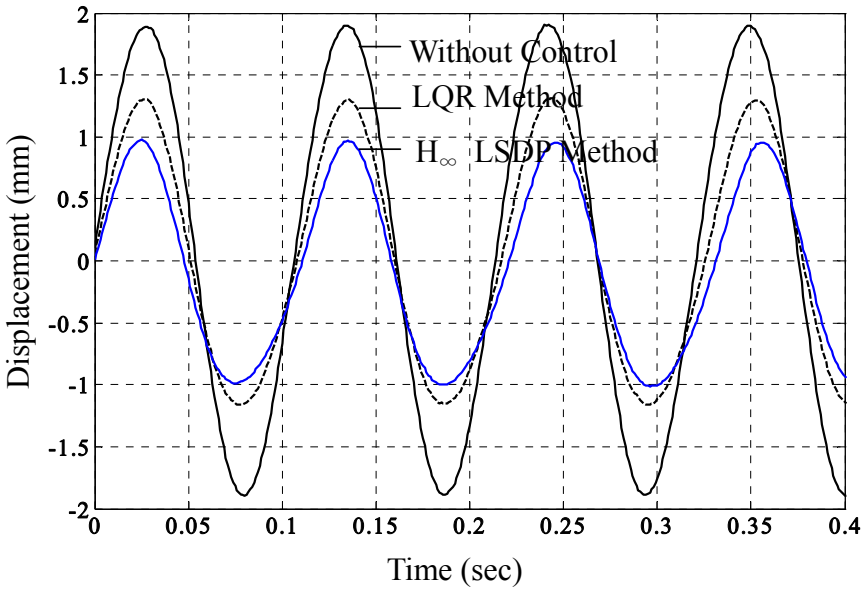

Fig. 5.15 Experimental result of displacement signal of the vibration body, the following system conditions: 1) disturbance frequency set to 59 rad/sec, 2) with feedback control, designed using LQR Method and 3) with feedback control, designed using H_∞LSDP Method

Figures 5.13, 5.14 and 5.15 revealed the experimental results for disturbance frequency of 5, 29 and 59 rad/sec. As a result, in the case without feedback control, the amplitude of the displacement signal from the vibration body was found to be higher than that with feedback control designed using the LQR method and H_∞ LSDP method.

Figure 5.16 shows the Bode diagram of the vibration control system. From the result, it can be observed that the gain of the displacement signal from the vibration body in the system with feedback control designed using the H_∞ LSDP method was lower than that designed using the LQR method and without feedback control.

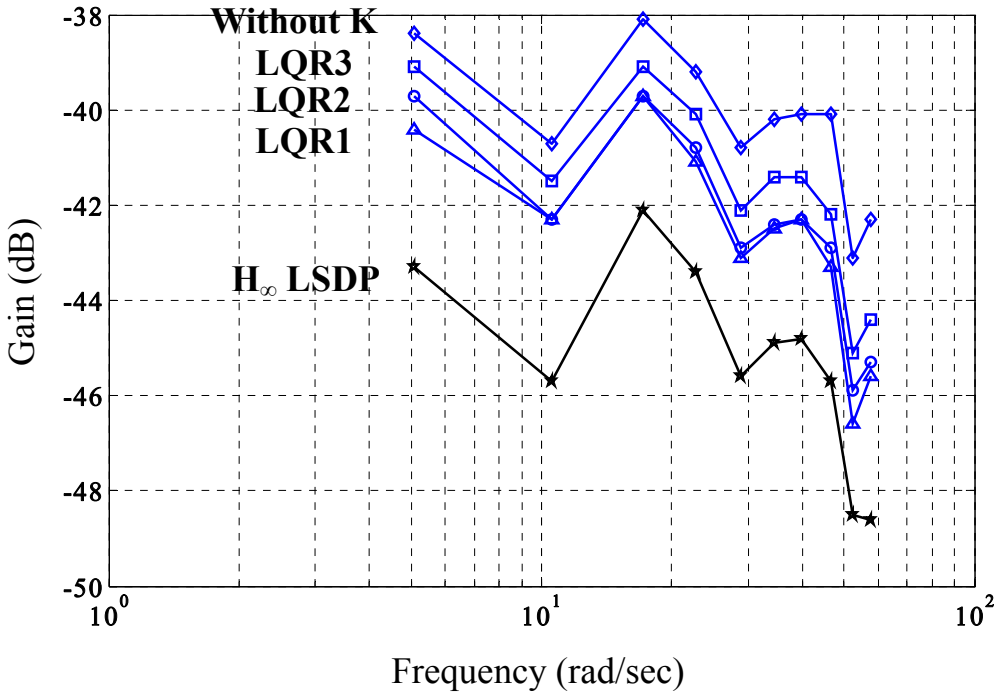

Fig. 5.16 Experimental result of Bode diagram of the displacement signal of the vibration body and the following system conditions: 1) without feedback control 2) with feedback control, gains set to LQR1 3) with feedback control, gains set to LQR2 4) with feedback control, gains set toLQR3 and 5) with feedback control, designed using H_∞LSDP Method

5.5 Conclusions

A vibration suppression control scheme based on linear actuator and permanent magnet is proposed in this chapter. The feedback control was designed using the H_∞LSDP Method. In this chapter, a model was set up for feasibility analysis; the system prototype was manufactured for experimental confirmation.

From the results of simulations and experiments, the following conclusions can be drawn:

- According to the model based on analysis of prototype performance, feedback control was achieved by closed-loop stability.
- Impulse response, the system with feedback controller could suppress the vibration of the object.
- Step response, the system with feedback controller could suppress in order to make the vibration object reach to the equilibrium position.
- Frequency response, at this view point the system has more effective than the feedback control that design using LQR method.

Chapter 6

Conclusions and recommendations

6.1 Conclusion

A vibration control system is the mechanism in which reduced object vibrating signal can be supported with noncontact active control. The advantage of such a system is that in the process of plating or rolling of steel sheets.

A noncontact vibration control in this research is suitable for the thin steel sheet rolling process. In this investigation, a noncontact magnet vibration system is controlled by the actuator to adjust the air gap between the permanent magnet and the vibration object is developed. In this system a permanent magnet is used to replace the electromagnet to make vibration control system. Compared with the electromagnet vibration control system, there is no force that generate by electromagnet system, due to system can suppress a large signal vibration from vibration objected, and no need coil space for electromagnet system.

6.2 Linear Quadratic Regulation (LQR) Approach

This research initially to demonstrate the vibration control system by means of LQR control theory, the LQR approach is the method of control for linear system. In this system, the nonlinear vibration control system is linearized.

Based the linearized system, in this study, the proposed vibration suppression mechanism is designed, the system prototype is constructed for experimental confirmations, feasibility of the model of prototype and the design of controller is analyzed.

Finally, the simulations and experimental results were verified that the system effectively suppressed vibration.

6.3 H_∞ Loop Shaping Approach

In this research, the optimal feedback control design by means of H_∞ Loop Shaping Design Procedure(LSDP), this method based on modern H_∞- optimization approach (H_∞-norm is maximum magnitude of frequency response), multivariable system, stability guaranteed in the face of plat perturbations and uncertainty, especial based on the concept of bode plot methods.

The examination results of the vibration control system that feedback control was designed by means of LSDP method shows the effective of controller.

6.4 Recommendation

The presented work of vibration control system in one-DOF system that still exists. Even though the vibration control system is successful in this research, the system modeling of the real-vibration object is need to find, in order to enlarge the potential field of the application, the existing set up should be improved on the following:

Further improvement of vibration type

Improvement of specification of measurement device

Improvement of alignment of the device

References

[1] Matsuda K., Yoshihashi M., Okada Y. and Tan ACC:Self-Sensing Active Suppression of Vibration of Flexible Steel Sheet, Trans. ASME, J. Vib. Acoust. Vol.118, pp. 469-473, 1996.

[2] Fujita M., Matsumura F. and Namerikawa T.: μ-Analysis and Synthesis of a Flexible Beam Magnetic Suspension System, Proc. 3rd Int. Symp. Magnetic Bearings, pp. 495-504, 1992.

[3] Stephens L.S., Timmerman M.A. and Casemore, M.A. :Gain Scheduled PID Control for Electromagnetic Vibration Absorbers, Proc. 6th Int. Symp. Magnetic Bearings, pp. 331-340, 1998.

[4] Betschon F. and Schob R., On-Line Adapted Vibration Control, Proc. 6th Int. Symp. Magnetic Bearings, pp. 362-371, 1998.

[5] Oka K. and Higuchi T.: Magnetic Levitation System by Reluctance Control: Levitation by Motion Control of Permanent Magnet Int. J. Applied Electromagnetics in Materials, Vol.4, pp. 369-375, 1994.

[6] Oka K. and Inoue Y.: Vibration Control With Linear Actuated Permanent Magnet: Proc. 6th Int. Conf. Motion and Vibration Control,vol.2, pp. 678-683, 2002.

[7] Allaire, P.E., Kasarda, M.E.F., Humphris, R.R., and Lewis, D.W. : Vibration Reduction in Multimass Flexible Rotor Using a Midspan Magnetic Damper, Proc. of the 1st Int. Simp. On Magnetic Bearings, ETH Zurich, Switzerland, pp. 149-158, 1988.

[8] Matsumura, F., Kido, M., Tanaka, Y., and Takeda, T.: Design Method of Horizontal Shaft Attractive Controlled Magnetic Bearings and its Characteristics, Trans IEE Japan, Vol,103, No. 3, pp. 130-137, 1983.

[9] Nagai B., Okada, Y., Matsuda, K., and Kibune, K.: Digital Control of Electro-Magnetic Damper for Rotating Machinery, Int. Conf, on Rotordynamics, Sept, 14-17, pp. 415-420, Tokyo, 1986.

[10] Oshinoya, Y., and Shimogo, T.: Electro-Magnetic Levitation Control of Traveling Elastic Plate, Proc of Int. Conf. On Advanced Mechatronics, May 21-24, Tokyo, pp. 845-850, 1989.

[11] Schweitzer, G., and Ulbrich, H.: Magnetic Bearings-A Novel Types of Suspension, Institution of Mechanical Engineering, Second Int. Conf. On Rotating Machinery, Cambridge, U.K., pp. C273-80, 1980.

[12] Zhang, H., Nagata, T., Okada Y., and Tani, J.,: Flexible Shell Structured Rotor Controlled by digital Magnetic Bearings, Tokyo, pp. 319-324, 1990.

[13] Kurita, Y., Sakurai, A., Hamazaki, Y., Ueda, H., H., Kato, K., and Kondo,H.: Suppression of Vibration on a Thin Steel Plate Using a Controlled Electromagnets, Proc. of the 1991 Asia-Pacific Vibration Conference, Melbourne, pp. 3.68, 1991.

[14] Okada, Y., Matsuda, K., and Hashiani, H.: Self-Sensing Active Vibration Control Using the Moving-Coil Type Actuators, ASME Journal of Vibration and Acoustics,Vol. 117, pp. 411-415, 1995.

[15] McFarlane D.C. and K. Glover, A loop shaping design procedure using H_∞ synthesis, IEEE Trans. On Automatic Control AC-37(6), pp. 759-769, 1992.

[16] McFarlane D.C. and K. Glover, An H_∞ Design Procedure using Robust Stabilization of Normalized Coprime Factors, Proc. 27th on Decision and Control, pp. 1343-1348, 1988.

[17] D.-W. Gu, P. Hr. Petkov and M.M. Konstatinov,: Robust Control Design with MATLAB:,Springer, London, 2005.

[18] Lanzon A, Simultaneous Synthesis of Weights and Controllers in H_∞ Loop-Shaping, Proc of 40th IEEE Conference of Decision and Control, pp. 670-675, 2001.

[19] McFarlane D.C. and K. Glover, Robust Controller Design Using Normalized Coprime Factor Plant Descriptions, Springer, New York, 1990.

[20] J.F. Whidborne, P. Pangalos, Y.H. Zweiri, and S.J. King: A graphical user interface for computer-aided robust control system design. Engineering Design Conf. 2002, pp. 383-392, London, July 2002.

[21] J. C. Doyle, :Analysis of feedback system with structured uncertainties, IEEE Proc., vol. 129-D, no.6, pp.242-250, 1982.

[22] M. Vidyasagar and H. Kimura, :Robust controllers for uncertain linear multivariable systems, Automatica, pp. 85-94, 1986.

[23] M. Vidyasagar, : The graph metric for unstable plants and robustness estimates for feedback stability, IEEE Trans. Automat., Contr., vol 29, pp. 403-417, 1984.

[24] G. stein and M. Athans, :The LQG/LTR procedure for multivariable feedback design, IEEE Trans. Automat., Contr., vol. 32, pp. 105-114, 1987.

[25] K. Zhou, J. C. Doyle, and K. Glover, :Robust and optimal control, Prentice Hall Inc., New Jersey, USA, 1996.

[26] Geir E. Dullerud and Fernando Paganini, :A course in Robust Control Theory, Springer, 1999.

[27] K. Zhou and J. C. Doyle, :Essentials of Robust Control. Englewood Cliffs, NJ, Printice-Hall, 1998.

[28] B. A. Francis, :A Course in H_∞ Control Theory, Lecture Notes in Control and Information Sciences, vol. 88, pp. 90-93, Springer-Verlag, 1987.

[29] A. Lazon, :Weight Optimization, in H_∞ Loop-Shaping, Automatica, vol. 41, no. 7, pp. 1201-1208, 2005.

[30] Ballois SL, Duc G, : H_∞ control of a satellite axis : Loop shaping controller reduction and μ -analysis. Contr. Eng. Practice, pp. 1001-1007, 1996.

[31] K. Glover, :All optimal Hankel-norm approximations of linear multivariable system and their $\mathcal{L}_\infty$-error bounds. International Journal of Control, 39(6), pp.1115-1193, 1984.

[32] A Lanzon, :Weight Selection in Robust Control: An Optimization Approach, PhD thesis, University of Cambridge, United Kingdom, October 2000.

[33] A. Lanzon and M. Cantoni, :A state-space algorithm for the simultaneous optimization of performance weights and controllers in μ -analysis, Proc of the 39th IEEE Conf. on Decision and control, Sydney, Australia, December 2000.

[34] A. Lanzon and R. J. Richards, : A frequency domain optimization algorithm for simultaneous design of performance weights and controllers in μ -analysis, Proc. of the 38th IEEE Conf. on Decision and control, Phoenix, Arizona, December 1999.

[35] G. Papageorgiou and K. Glover. :A systematic procedure for designing non-diagonal weights to facilitate H_∞ loop-shaping, Proc of the 36th IEEE Conf. on Decision and control, San Diego, CA, 1997.

[36] G. Papageorgiou and K. Glover. : H_∞ loop-shaping: Why is it a sensible procedure for designing robust flight controllers?, Proc. of the AIAA Conf. on Guidance, Navigation and control, August 1999.

[37] J. F. Whidborne, I. Postlethwaite and D. W. Gu, : Robust Controller Design Using H_∞ loop-shaping and the Method of Inequalities, IEEE Trans. Control Systems Technol., vol. 14, pp. 602-604, 1981.

[38] B.A. Francis. :A Course in H_∞ control Theory, vol. 88 of Lecture Note in control and information Sciences, Springer-Verlag, 1987.

[39] D. W. Gu, P. Hr., Petkov, and M. M. Konstantinov., :Direct Formular H_∞ loop-shaping design procedure controllers, Proc. of the 15th IFAC World Congress, paper 276, session T-Mo-M15, Barcelona, Spain, July 2002.

[40] D. Hoyle, R. Hyde, and D. J. N. Limebeer, : An H_∞ approach to two-degree-of-freedom design, Proc. of the 30th IEEE Conf. on Decision and Control, pp. 1581-1585, Brighton, UK, 1991.

[41] http://www.maruichikokan.co.jp/product/process.html

[42] Shinko Electric co, LTD,: Electromagnet Vibration Control System for Steel Sheet, http://www.shinko-elec.co.jp/NewsReleases/new_18.htm

List of publications

Publication of Journal

[1] Phaisarn SUDWILAI, Koichi OKA, Akiyuki SANO and Yuta HIROKAWA; ***Vibration Control With Linear Actuator Permanent Magnet System using LQR Method***; Journal of System Design and Dynamics, Vol.5, No.6 (2011), pp.1-13

[2]Phaisarn SUDWILAI and Koichi OKA; ***The Frequency Response of Vibration Control With a Linear Actuator and a Permanent Magnet***; Journal of the Japan Society of Applied Electromagnetics and Machanics, Vol. 20, No.2 (June 2012), pp 526-531

Publication for International Conference

[3]Phaisarn SUDWILAI, Koichi OKA, Akiyuki SANO and Yuta HIROKAWA: ***"Vibration Control With Linear Actuator Permanent Magnet System using Robust Control"***, The 10th International Conference on Motion and Vibration Control, Tokyo, Japan, 2010, No.10-203, pp.1-11

[4]Phaisarn SUDWILAI, Koichi OKA and Yuta HIROKAWA; ***"Frequency Response of Vibration Control With Linear Actuator and Permanent Magnet"***, The 20th MAGDA Conference in Pacific Asia, Taiwan, November 14-16, 2011

[5]Phaisarn SUDWILAI, Koichi OKA and Yuta HIROKAWA: ***"Vibration Control of Parallel Spring Using Linear Actuator and Permanent Magnet"***, The 4th Thailand-Japan International Academic Conference , November 26-27, 2011, Tokyo, Japan (best presentation awards)

[6]Phaisarn SUDWILAI and Koichi OKA: ***"Vibration Control with Linear Actuator Permanent Magnet System using Robust Control"***, the 2012 Asia-Pacific Symposium on Applied Electromagnetics and Mechanics, July 25-27, 2012, Ho Chi Minh, Vietnam

Publication for Domestic Conference

[7]Phaisarn SUDWILAI, Koichi OKA and Yuta HIROKAWA: ***"Vibration Control With Linear Actuator and Permanent Magnet",*** The 16th Intelligent Mechatronics Workshop , September 2-3, 2011, Kochi, Japan

Acknowledgements

The author wishes to express his profound gratitude and to respectfully dedicate this work to his parent and family members for their endless encouragements, love and sacrifices. The author is most grateful to his advisor, Prof. Dr. Koichi OKA, for his valuable supervision, supports and encouragements throughout the study. Grateful acknowledgements are also made to Prof. Dr. Yoshio INOUE, Prof. Dr. Shuoyu WANG, Prof. Dr. Fumiaki TAKEDA and Prof. Dr. Kyoko SHIBATA, members of thesis committee, for their valuable suggestions and comments.

The author wishes to acknowledge Prof. Lawrence Hunter for his valuable guidance in research writing, and to Prof. Ban Mikiko, Mr. Yoshida Motori, Ms. Kubo Mariko, Ms. Kiyooka Kimi, Ms. Fukudome Sonoko, Ms. Sakamoto Kimiko, Ms. Yamasaki Mari, and Ms. Fujii Rika, members of International Relation Center, for their administrative supports and Japanese language instructions. The author also wishes to acknowledge Kochi University of Technology for a great opportunity of PhD study and financial supports under Special Scholarship Program.

The author sincerely appreciates his parents, family members, Ms Amornrat Booncherdchu and all of his Thai friends in Kochi and Japan for their friendships and goodwill. Sincere appreciate also Japanese friends in OKA-Laboratory for their useful technical experience sharing and kind technical assistance, especially Mr. Kunihiko TACHIBANA.